Biogeochemistry (2009) 95:37–59
DOI 10.1007/s10533-008-9233-4

ORIGINAL PAPER

Biological and physical influences on the carbon isotope content of CO_2 in a subalpine forest snowpack, Niwot Ridge, Colorado

D. R. Bowling · W. J. Massman · S. M. Schaeffer · S. P. Burns · R. K. Monson · M. W. Williams

Received: 27 May 2008 / Accepted: 8 August 2008 / Published online: 9 September 2008

Abstract Considerable research has recently been devoted to understanding biogeochemical processes under winter snow cover, leading to enhanced appreciation of the importance of many winter ecological processes. In this study, a comprehensive investigation of the stable carbon isotope composition ($\delta^{13}C$) of CO_2 within a high-elevation subalpine forest snowpack was conducted. Our goals were to study the $\delta^{13}C$ of biological soil respiration under snow in winter, and to assess the relative importance of diffusion and advection (ventilation by wind) for gas transport within snow. In agreement with other studies, we found evidence of an active microbial community under a roughly 1-m deep snowpack during winter and into spring as it melted. Under-snow CO_2 mole fractions were observed up to 3,500 μmol mol^{-1}, and $\delta^{13}C$ of CO_2 varied from ~ -22 to ~ -8‰. The $\delta^{13}C$ of soil respiration calculated from mixing relationships was -26 to -24‰, and although it varied in time, it was generally close to that of the bulk organic horizon (-26.0‰). Subnivean CO_2 and $\delta^{13}C$ were quite dynamic in response to changes in soil temperature, liquid water availability, and wind events. No clear biologically-induced isotopic changes were observed during periods when microbial activity and root/rhizosphere activity were expected to vary, although such changes cannot be eliminated. There was clear evidence of isotopic enrichment associated with diffusive transport as predicted by theory, but simple

D. R. Bowling (✉) · S. M. Schaeffer
Department of Biology, University of Utah, 257 South 1400 East, Salt Lake City, UT 84112-0820, USA
e-mail: bowling@biology.utah.edu

W. J. Massman
Rocky Mountain Research Station, USDA Forest Service, Fort Collins, CO, USA

Present Address:
S. M. Schaeffer
Department of Ecology, Evolution, and Marine Biology, University of California, Santa Barbara, CA 93106, USA

S. P. Burns
Department of Ecology and Evolutionary Biology, University of Colorado, Boulder, CO 80309, USA

S. P. Burns
National Center for Atmospheric Research, Boulder CO 80307, USA

R. K. Monson
Department of Ecology and Evolutionary Biology, University of Colorado, Boulder, CO 80309, USA

R. K. Monson
Cooperative Institute for Research in Environmental Sciences, University of Colorado, Boulder, CO 80309, USA

M. W. Williams
Institute of Arctic and Alpine Research and Department of Geography, University of Colorado, Boulder, CO 80309, USA

diffusive enrichment (4.4‰) was not observed. Instead, ventilation of the snowpack by sustained wind events in the forest canopy led to changes in the diffusively-enriched gas profile. The isotopic influence of diffusion on gases in the snowpack and litter was greatest at greater depths, due to the decreased relative contribution of advection at depth. There were highly significant correlations between the apparent isotopic content of respiration from the soil with wind speed and pressure. In summary, physical factors influencing gas transport substantially modified and potentially obscured biological factors in their effects on $\delta^{13}C$ of CO_2 within this subalpine forest snowpack.

Keywords Carbon dioxide · Microbial · Niwot Ridge AmeriFlux site · Soil respiration · Stable isotope · Winter

Introduction

The presence of enhanced carbon dioxide concentration under snow attributed to winter biological activity has been known for several decades (Kelley et al. 1968). A wide variety of organisms inhabit the snow surface, snowpack, and subnivean soil, including bacteria, cyanobacteria, algae, and fungi (Hoham and Duval 2001), as well as invertebrates, birds, small mammals (Aitchison 2001), plants and plant roots. While ecologists used to think of winter as a relatively dormant season, there is a growing appreciation of the importance of many ecological processes in winter (e.g., Schmidt and Lipson 2004). In temperate coniferous forests there can be substantial carbon gain outside what is traditionally thought of as the "growing season" (Anthoni et al. 1999), and many forests begin to gain carbon a month or more before the snow is fully melted (Monson et al. 2005; Suni et al. 2003). Winter respiration can be a significant fraction of the annual carbon budget in many ecosystems (reviewed by Brooks et al. 2005). Mass loss of litter in winter can be 50–90% of annual litter fall (Coxson and Parkinson 1987), and winter litter decomposition rates in high elevation subalpine forests can exceed those in summer (Kueppers and Harte 2005). When liquid water is available, microbial activity is possible at subfreezing temperature as low as −6°C (Brooks et al. 1996; Edwards and Cresser 1992; Mikan et al. 2002; Schmidt et al. 2008) with some evidence for activity at −39°C (Panikov et al. 2006). Microbial dynamics can be altered by freeze-thaw cycles (Lipson and Monson 1998; Matzner and Borken 2008; Schimel and Clein 1996). In some circumstances the heat produced by microbial metabolism can lead to isolated and relatively warm pockets of activity even when surrounding soils are very cold (Zimov et al. 1993). The taxonomic composition of the bacterial and fungal communities in the soil can be substantially different in winter and summer (Lipson 2007; Monson et al. 2006b; Schadt et al. 2003). In some locations microbial biomass is higher in winter than during the summer growing season (Lipson et al. 2000; Schadt et al. 2003). Interest in these biogeochemical processes during winter has led to a large body of research focused on the fluxes of CO_2 from snow-covered ecosystems (Groffman et al. 2006; Hirano 2005; Mariko et al. 2000; Mast et al. 1998; McDowell et al. 2000; Monson et al. 2006b; Musselman et al. 2005; Oechel et al. 1997; Schindlbacher et al. 2007; Suzuki et al. 2006; Takagi et al. 2005; Uchida et al. 2005).

Carbon isotopes have been tremendously useful in process-level ecological studies (see review by Bowling et al. 2008). Most of our understanding of the isotopic composition of whole-forest respiration (commonly called δ_R or $\delta^{13}C_R$, see Table 1 for a list of symbols) in temperate regions comes from research conducted in the warmer summer months (Alstad et al. 2007; Bowling et al. 2002; Hemming et al. 2005; Knohl et al. 2005; Lai et al. 2005; McDowell et al. 2004; Mortazavi et al. 2005; Ponton et al. 2006), and we have little isotopic understanding of winter processes. This is primarily due to a limitation of the technique used to assess δ_R, which is an isotopic mixing relationship involving measurements of $\delta^{13}C$ and CO_2 in forest air (described below). The problem is illustrated in Fig. 1, which shows a 1-year period of CO_2 and $\delta^{13}C$ observed in air at a subalpine forest in Colorado, USA (the Niwot Ridge forest, location of the present study). Warmer temperature in the summer leads to enhanced biological activity, and there is considerable variation in CO_2 in the forest in summer as a result, both with time and with height. Winter is much colder and windier, and there is far less variation in CO_2, leading

Table 1 List of symbols used in the text

CO_2, C_a	Carbon dioxide mole fraction in air (μmol CO_2 mol^{-1})
$\delta^{13}C$	Carbon isotope composition of organic material or CO_2 (‰)
C_s	CO_2 mole fraction in soil or snow gas (μmol CO_2 mol^{-1})
C_a^{12}	$^{12}CO_2$ mole fraction in air (μmol $^{12}CO_2$ mol^{-1})
C_s^{12}	$^{12}CO_2$ mole fraction in soil or snow gas (μmol $^{12}CO_2$ mol^{-1})
δ_S	$\delta^{13}C$ of CO_2 in soil or snow gas (‰)
δ_a	$\delta^{13}C$ of CO_2 in air (‰)
δ_J	$\delta^{13}C$ of soil respiration flux, calculated using Eq. 2 (‰)
δ_R	$\delta^{13}C$ of whole-forest respiration, calculated from a Keeling plot intercept using measurements made from air inlets (‰)
δ_{R*}	Apparent $\delta^{13}C$ of under-snow respiration, from a Keeling plot using different combinations of inlets on each profile separately as follows (‰)
	$\delta_{R*,a}$ All air and snow inlets on the profile
	$\delta_{R*,b}$ All air, snow, and litter surface inlets on the profile
	$\delta_{R*,c}$ All air, snow, litter surface, and within-litter inlets on the profile

See Fig. 3 for a related diagram

to seasonal patterns that are observed in most temperate forests (e.g., Murayama et al. 2003).

Because forest respiration and photosynthesis influence both CO_2 and $\delta^{13}C$, there is a less-well-known but related seasonal pattern in $\delta^{13}C$ of forest air (Fig. 1b). The intercept of a regression of $\delta^{13}C$ versus $1/CO_2$ (a Keeling plot) is commonly used to determine the isotope ratio of forest respiration. Because of the large ranges in CO_2 and $\delta^{13}C$ in summer, δ_R can be determined with a high degree of confidence. In winter, the small ranges lead to large uncertainty in the mixing relationships and unrealistic values of δ_R (Fig. 1c, which is derived from the data in Fig. 1a, b). This limitation of the regression-based technique has been described in detail by Zobitz and colleagues (2006). Studies which have reported winter δ_R values from a variety of forests (Lai et al. 2005; McDowell et al. 2004) have reported similar results. Hence, our understanding of CO_2 isotopes associated with winter processes lags compared to our understanding of summer processes.

Carbon isotopes of respiratory fluxes contain information about the origin of the carbon in those fluxes. There are systematic differences in $\delta^{13}C$ of plant and soil organic materials, for example between labile sugars, cellulose and lignin, bulk (humified) soil organic matter, root, mycorrhizal, or saprotrophic fungal biomass, and the respiratory fluxes associated with transfers between these pools (Bowling et al. 2008). Based on these differences, a shift from more labile to more recalcitrant respiratory substrates, or from winter dominance of heterotrophic activity to enhanced autotrophic respiration during spring thaw might be discernible based on $\delta^{13}C$ of soil respiration under snow. Given the importance of winter microbial activity to ecosystem carbon budgets discussed above, and the importance of the isotopic composition of terrestrial respiration to studies of the carbon cycle at larger scales (Chen et al. 2006; Randerson et al. 2002; Scholze et al. 2008; Suits et al. 2005), research is needed to determine the primary biological, physical, and chemical controls on $\delta^{13}C$ of respiration in winter.

Little research has been conducted on CO_2 isotopes in snow, but several studies have focused on CO_2 isotopes in firn due to their importance in paleoclimatological studies (Assonov et al. 2005; Clark et al. 2007; Francey et al. 1999; Trudinger et al. 1997). Some of this theory is relevant to CO_2 isotopes in snowpacks, but there are differences that prevent direct application of theory and models from these studies to forest snowpacks. For example, the influence of advection is limited to the very surface of the firn, but it is important throughout a forest snowpack as we will show.

We are aware of two studies that have reported measurements of CO_2 isotopes within forest snowpacks (Brooks et al. 2005; Cerling et al. 1991). Although focused primarily on soil processes, the paper by Cerling and colleagues was important because it described the governing isotope effects associated with diffusion in soils (and snow), and showed that the carbon isotope content of CO_2 within the soil (or snow) gas differs from that which leaves the surface as a flux (see also Amundson et al. 1998; Davidson 1995). The theoretical expectations for CO_2 isotope effects within the snowpack resulting from steady state diffusion theory are illustrated in Fig. 2. Panel (a) shows the mixing relationships between the measured quantities $\delta^{13}C$ and CO_2, and panel (b) shows the mixing lines in $1/CO_2$ (Keeling plot) space. CO_2 in air will mix with a respiratory source of arbitrary but constant isotope ratio δ_J along the solid

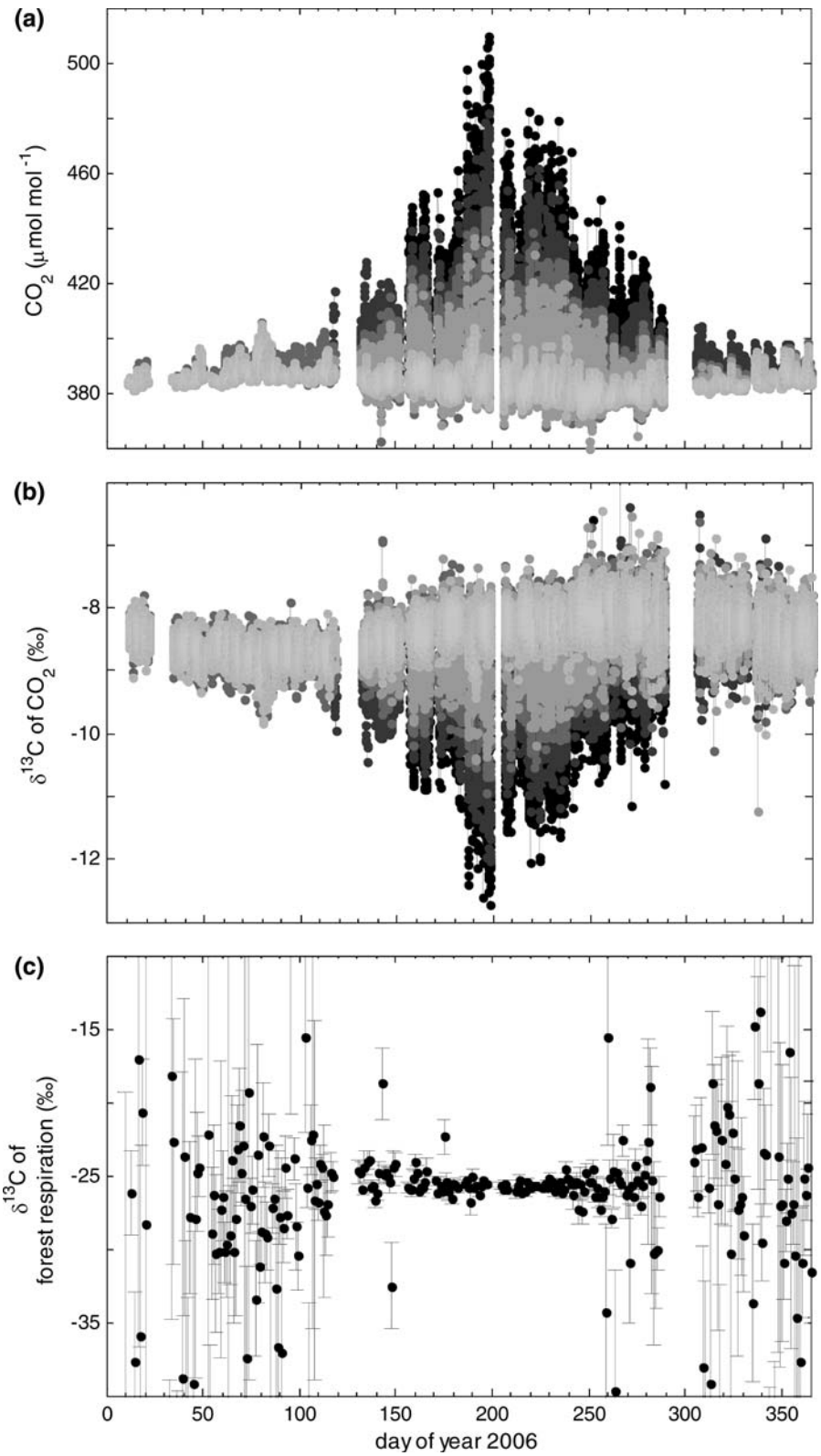

Fig. 1 (**a**) CO_2 and (**b**) $\delta^{13}C$ of CO_2 in forest air at several heights (0.1, 1, 5, 7, 21.5 m) during 2006. Observations within the snowpack are not included in this figure. Colors are darkest to lightest from lowest inlet to highest. (**c**) The carbon isotope content of nocturnal whole-forest respiration (δ_R), calculated as a Keeling plot intercept of the data in panels (**a**) and (**b**) for each day of year. Error bars are the standard error of the intercept. Data were collected as described by Schaeffer et al. (in press) and are previously unpublished

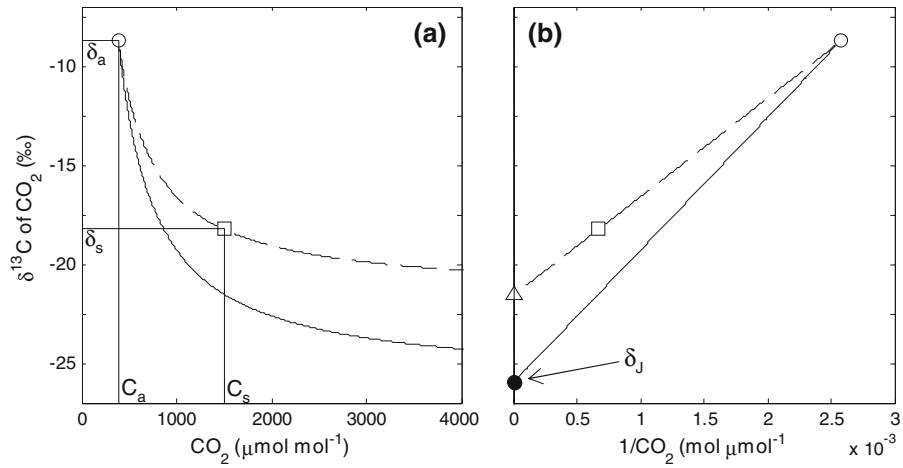

Fig. 2 Theoretical mixing relationships between $\delta^{13}C$ and CO_2 within the snowpack. Panel (**a**) shows the mixing lines as they apply to measurable quantities and (**b**) shows the same in $1/CO_2$ space. The open circle corresponds to the $\delta^{13}C$ and CO_2 (or $1/CO_2$) of the air above the snowpack (C_a and δ_a), the open square represents these quantities measured within the snowpack (C_s and δ_s), and the black circle corresponds to the $\delta^{13}C$ of respiration (δ_J from Eq. 2). The solid line (both panels) shows a mixing line between the air and the respiratory source (which would occur only in the absence of diffusion). The open triangle corresponds to an enrichment of 4.4‰ relative to the respiratory source δ_J, and the dashed line (both panels) shows a mixing line of this enriched source with the air (described by Eq. 2). The mixing lines in (**a**) are asymptotic to the black circle and open triangle at infinite CO_2. Values shown for CO_2 in air (*open circle*) are the means measured at 120 cm during this study, which were 388.4 μmol mol^{-1} and −8.7‰

line (Keeling 1958). In the absence of diffusion, any increase in CO_2 caused by respiration, or decrease in CO_2 caused by ventilation of the snowpack with air, will occur along the solid line. However, due to the difference in mass of the isotopic variants $^{16}O^{12}C^{16}O$ and $^{16}O^{13}C^{16}O$, their binary diffusivities in air differ (diffusive transport of the lighter isotope is greater than that of the heavy isotope). Diffusion will cause an enrichment of the gas within the snow (or soil) profile of 4.4‰ (enrichment means the gas contains relatively more of the heavy isotope, and $\delta^{13}C$ becomes less negative). Theory that relates the 4.4‰ factor to molecular mass was provided by Cerling et al. (1991). Hence, under fully diffusive transport, gas within the snow should follow the dashed mixing lines shown in Fig. 2 (the open triangle is enriched by 4.4‰ from the black circle). The curved lines in Fig. 2a show the same phenomena, and mixing under the two extreme cases (no diffusion or purely diffusive) will follow the solid and dashed mixing lines, respectively. The lines in Fig. 2a are asymptotic to the black circle and open triangle, and reach them at infinite CO_2 (where $1/CO_2 = 0$ on Fig. 2b). To the extent that advection (ventilation of the snowpack with air from the atmosphere) influences transport, and depending on the time required for a fully diffusive profile to establish, actual measurements of $\delta^{13}C$ and CO_2 in snow may fall within the two extreme cases.

We conducted a field study in a high-elevation subalpine forest in winter to address two objectives. Our first goal was to quantify the isotopic composition of soil respiration in a subalpine forest in winter and evaluate potential biological controls on the $\delta^{13}C$ of winter respiration. Second, we examined the $\delta^{13}C$ content of CO_2 in the snowpack in the context of diffusive and advective transport. Although sophisticated physical gas transport models can be applied to investigate these processes (Massman 2006; Massman and Frank 2006; Massman et al. 1997; Monson et al. 2006a), we limit our focus in this paper to description and interpretation of the observations. We will address the more quantitative aspects of CO_2 isotopic transport in snowpacks in a future paper.

Methods

Study location

This study was conducted during February–June 2007 in a subalpine forest (the Niwot Ridge

AmeriFlux tower site, 40.03 °N, 105.55 °W, 3,050 m elevation) in the southern Rocky Mountains of Colorado, USA. The approximately 110-year old forest is dominated by three conifer species, *Pinus contorta*, *Picea engelmannii*, and *Abies lasiocarpa*. The mean annual temperature is 1.5°C, and the mean annual precipitation is 800 mm. Average peak snow water equivalence (SWE) is 328 mm on April 21 (1971–2000, National Resources Conservation Service, http://www.wcc.nrcs.usda.gov/snotel/). Snow cover at the site generally lasts from October/November through May/June. Further site details are available elsewhere (Monson et al. 2002, 2005, 2006a; Sacks et al. 2007).

Gas sampling and carbon isotope measurements

This work builds on previous studies that have examined $\delta^{13}C$ of CO_2 in air at the Niwot Ridge forest (Alstad et al. 2007; Bowling et al. 2005; Schaeffer et al. 2008, in press; Zobitz et al. 2006, 2007, 2008). For the present study, measurements of CO_2 mole fraction and $\delta^{13}C$ of CO_2 were made in the snowpack, the litter, and the air from February 9 until the snow fully melted on June 15, 2007 (DOY 40-166). Samples were measured by pumping gas from the inlet locations (described below) through 38–40 m of 0.64 cm dia. tubing (Type 1300, Synflex Specialty Products, Mantua, Ohio) to a tunable diode laser (TDL) absorption spectrometer (TGA100A, Campbell Scientific, Inc., Logan, Utah). The TDL system at the Niwot Ridge forest has been described in detail by Schaeffer et al. (in press). CO_2 data are World Meteorological Organization-traceable and $\delta^{13}C$ data are presented using standard notation (Farquhar et al. 1989) relative to the Vienna PDB scale, both accessed via standards in our laboratory at the University of Utah.

For the snowpack application, a sampling manifold was designed to dilute the relatively high mole fraction gas in the snowpack (up to 4,000 µmol mol^{-1}) to a measurable range for the instrument (350–600 µmol mol^{-1}). This consisted of two mass flow controllers (Type 1179A, MKS Instruments, Andover, Massachusetts) which mixed CO_2-free air (generated by pumping air through a soda lime trap) with sample gas at controlled flow rates. Gas was sampled from inlet locations at 225–300 ml min^{-1} (all flow rates at STP), and was mixed with CO_2-free air at variable flow rates, which were determined and controlled using a datalogger (CR5000, Campbell Scientific, Inc., Logan, Utah). The influence of the dilution system on the precision and accuracy of the gas measurements was not assessed, although automated tests were made daily to insure that the mixing air stream was CO_2-free. The analytical precision for the analyzer during this period was 0.2 µmol mol^{-1} for $[CO_2]$ and 0.35‰ for $\delta^{13}C$ (Schaeffer et al. in press).

Air from two snowpack vertical profiles was measured, located within 30 m of the Niwot Ridge flux tower with a horizontal separation of 6.5 m between profile 1 and profile 2. Profiles and tubing were installed in the fall and the natural snowpack formed around them without disturbance. CO_2 measurements from the profiles began in midwinter. Each profile (see Fig. 3) comprised 8 inlets located at these sampling heights relative to the litter surface: −3 cm (within the O-horizon), 0 (litter surface), 20, 40, 60, 80, 100, and 120 cm (the higher inlets were sometimes/always in the air and not the snowpack). Inlets were 10 cm dia. × 1 cm tall stainless steel cylinders that were covered on top and bottom with 61 µm stainless steel mesh (Sommerfeld et al. 1991), and a

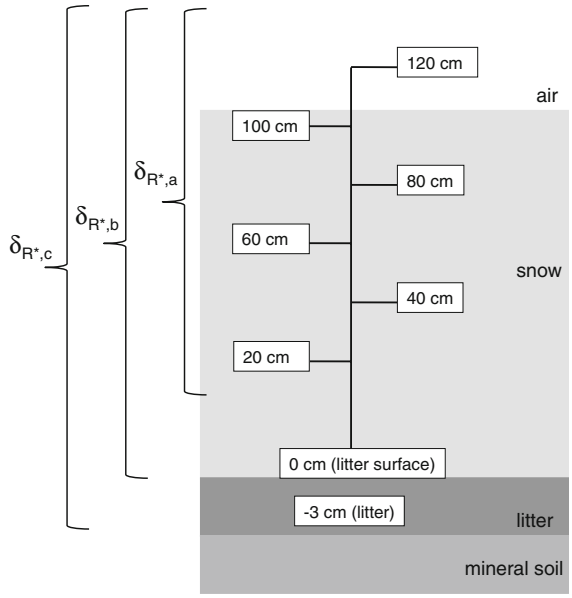

Fig. 3 A diagram of the sampling profile assembly showing how different subsets of inlets were grouped to calculate the apparent $\delta^{13}C$ of under snow respiration (δ_{R*}) for each profile frame. Snow depth varied during the study and sometimes the lower inlets were also in the air

filter (1.0 μm PTFE, Acro-50, Pall Corporation, East Hills, New York). Each profile assembly was made of a frame of wooden dowels held together with hose clamps. Samples above the ground (20–120 cm) were located at alternate sides of the frame, so that the 20, 60, and 100 cm locations were along one vertical axis and the 40, 80, and 120 cm locations were along a second vertical axis, with the two axes on each frame separated by ~1 m horizontally. The 0 and −3 cm locations were located on either side of the frame horizontally within 40 cm of the center. Sample tubing was routed along the ground (under the snowpack) to the analyzer and was not heated. The location of the sampling tubing at the bottom of the snowpack and resulting temperature equilibration removed the need for density corrections due to variation in gas temperature. Air was not dried before entry into the manifold/dilution system, but was dried before entry into the TDL using a Nafion counterflow assembly (PD 625, Campbell Scientific, Inc., Logan, Utah).

The sampling strategy was designed to minimize disruption of the diffusive profile within the snowpack. During the second half of every hour, measurements were made of the gases from 6 of the 16 snowpack inlets for 5 min each. (The first half of every hour, the TDL was used to measure vertical profiles in air as shown in Fig. 1.) Sample gas was pumped at 300 ml min^{-1} for 3 min (while calibration gases were being measured), then at 225 ml min^{-1} for 2 min, for a total volume of 1.35 l sampled from each inlet over 5 min. During the latter 2-min period gas was routed to the TDL analyzer (to verify stability of the CO_2), and the last 10 s of this period were averaged as a measurement. A full cycle of all 16 inlets on the two profiles was completed in three half-hour periods, so each inlet was idle for 2 h and 55 min, and flowed as described above for 5 min. Assuming that the sampling disrupted a sphere of gas surrounding the inlet, a sampled volume of 1.35 l would disrupt the mole fraction gradient in a radius of 6.9 cm (13.8 cm dia.) surrounding the inlet. A typical diffusion coefficient for CO_2 in soil or snow is 0.05 to 0.1 cm^2/s (Albert and Shultz 2002; Solomon and Cerling 1987), and it would take $t = x^2/4D = (13.8)^2/(4 \times 0.1) = 476$ s (7.9 min) for planar diffusion to reestablish the gradient (Nobel 2005). In subsequent experiments we re-measured several inlets 25 min after the initial measurement for several winter and summer months, and found no difference in CO_2 or $\delta^{13}C$ upon re-measurement (data not shown). Thus the advective influence of our sampling was negligible.

Meteorological and hydrological measurements

Temperature (snow, litter, or air) was monitored at all gas inlets using type T thermocouples. A diel artifact caused by heat conduction through the thermocouple wire was identified after the study, and was removed by filtering the data using a low-pass (4-h) window then using daily means of the filtered data. Comparisons with independent temperature measurements verified the suitability of this correction (data not shown). Soil temperature was also monitored using platinum resistance thermometers (STP-1, Radiation Energy Balance Systems, Seattle, WA) at 5 and 15 cm depths in a pit located ~60 m from the profiles.

Soil moisture was measured at 3 surface locations within 1 m of the profiles and within the pit described above using water content reflectometers (0–10 cm depth, CS615 and CS616, Campbell Scientific, Inc., Logan, Utah), and a second set of dielectric-based sensors (0–6 cm depth, Hydra-probes, Stevens Water Monitoring Systems, Portland, OR). Soil moisture data are used to indicate the timing of changes in the amount of liquid water in the surface soil and are presented on a relative scale, zeroed on DOY 60. SWE (using a snow pillow) and snow depth (ultrasonic depth sensor) were monitored continuously ~400 m from the site by the National Resources Conservation Service SNOTEL Program (http://www.wcc.nrcs.usda.gov/snotel/). Snow pits were excavated and sampled by hand at representative locations within 15 m of the profiles approximately every 10 days during the study, following the protocols of Williams et al. (1999). Measurements included density, SWE, and snow temperature profiles (every 10 cm), total snow depth, and grain size.

Additional meteorological data and whole-forest CO_2 flux data (using eddy covariance) were obtained from the ongoing Niwot Ridge AmeriFlux tower measurement program as described elsewhere (Monson et al. 2002).

Isotopic mixing relationships

Two mixing approaches were used. First, the Keeling plot approach (Keeling 1958; Pataki et al. 2003) was used to infer the isotopic composition of nocturnal whole-forest respiration (δ_R) or the isotopic composition of the apparent respiratory source in the snowpack (which we denote δ_{R*} in this paper). δ_R data are presented in Fig. 1 only, and the remainder of the paper is focused on δ_{R*}. Regressions were performed of $\delta^{13}C$ versus $1/[CO_2]$, and the intercept of the regression line was taken as δ_R or δ_{R*}, with the standard error of that intercept used as a measure of uncertainty. Following the recommendations of Zobitz et al. (2006), and contrasting with most previous studies, ordinary least squares (Type I) regressions were used. No outliers were removed from the Keeling plots. Time periods assessed varied from 3 to 48 h. Depending on the time period, calculations of δ_{R*} sometimes involved both daytime and nighttime observations. Regressions were performed with observations from air inlets only (8 pm to 4 am, to compute δ_R), or various combinations of air, snowpack, litter surface, and within-litter inlets (various time periods, to compute δ_{R*}, as described in Fig. 3 and Table 1). Note that δ_{R*} will not match δ_R under most conditions due to the influence of diffusive fractionation in the snowpack.

The second mixing approach follows Davidson (1995), who provided a derivation for the following equation relating observations of CO_2 and $\delta^{13}C$ in air and in the soil (or snow) gas

$$\delta_s = 1.0044\delta_J + \frac{C_a^{12}}{C_s^{12}}(\delta_a - 1.0044\delta_J - 4.4) + 4.4‰ \quad (1)$$

where C_a^{12} and C_s^{12} are the $^{12}CO_2$ mole fractions (μmol $^{12}CO_2$ mol^{-1}) in the air and in the soil (or snow) gas, respectively, δ_a and δ_s are the $\delta^{13}C$ of CO_2 in the air and in the soil gas, and δ_J is the $\delta^{13}C$ of the respiration flux leaving the soil surface. Since CO_2 is almost 99% $^{12}CO_2$, the ratio C_a^{12}/C_s^{12} can be replaced by total CO_2 (the sum of $^{12}CO_2 + {}^{13}CO_2$ for each, represented by C_a and C_s) with only a small resulting error in δ_s (<0.001‰). Making this approximation and solving for δ_J we obtain

$$\delta_J = \frac{C_s(\delta_s - 4.4) - C_a(\delta_a - 4.4)}{1.0044(C_s - C_a)}‰ \quad (2)$$

Equation 2 provides a means to obtain the isotope ratio of soil respiration (δ_J) from measurements of CO_2 and $\delta^{13}C$ made at two locations, in the air and within the soil (or snowpack). In this paper we present δ_J obtained from measurements in the air at 120 cm and at the soil–snow interface. There are several assumptions made in deriving this equation (Davidson 1995). First, it is applicable only for purely diffusive transport (a condition which is often violated as we will show) under steady state conditions. At the soil–air (or snowpack–air) interface, the mole fractions of CO_2 must be equal ($C_s = C_a$ at the interface), and a no-flux boundary is assumed at depth in the soil. The ratio of production of $^{12}CO_2$ and $^{13}CO_2$ is assumed to be the same at all depths in the soil. Last, the $\delta^{13}C$ of the biological respiratory flux must equal the physical flux from the surface to the air. Equation 2 describes the upper line in Fig. 2b, which connects the air (open circle) and the soil gas (open square), and from these measurements one can obtain δ_J. Alternatively, if data are available at multiple depths, a Keeling plot may be used to define the upper line in Fig. 2b, and δ_J can be obtained by subtracting 4.4‰ from the intercept ($\delta_{R*} - 4.4$). Equation 2 is a two-point variant of the Keeling plot approach.

Results and discussion

Environmental conditions, CO_2 and isotopes within the snowpack

The environmental conditions during the study are shown in Fig. 4. At the end of January, air temperature was cold, as low as −24°C. Minimum snow temperature of about −4°C occurred at that time. A fairly deep snowpack developed in the late fall and the snowpack depth was greater than 1 m at the beginning of CO_2 measurements (Fig. 4d), so the mineral soil temperature during the study was fairly warm, always above 0°C. Temperature of the litter layer during the study ranged from −0.5 to 0.75°C. A period of successively warm days resulted in isothermal conditions across the snowpack, and the appearance of

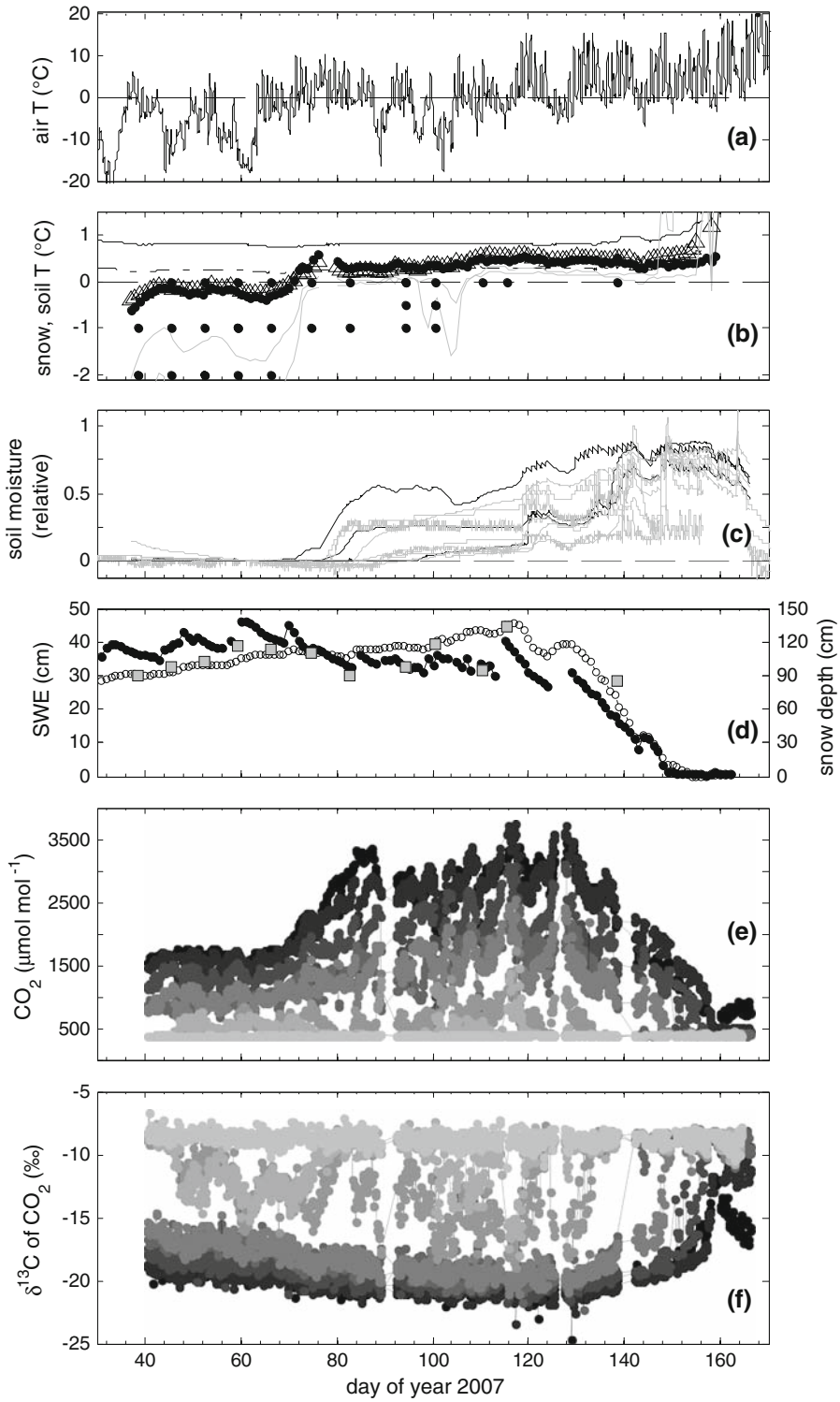

Fig. 4 Environmental conditions, CO_2, and $\delta^{13}C$ within the litter, snowpack, and air during the study. (**a**) air temperature (T) at 2 m, (**b**) mineral soil T at −15 cm (*solid thin line*) and −5 cm (*dot-dash line*), litter T at −3 cm (*triangles*), litter surface T (*continuous black circles*), snow T at 30 and 60 cm (*gray lines*), and snow T within hand-dug pits at depths less than 60 cm (*black circles*), (**c**) relative soil moisture content (zeroed on day 60) at 0–10 cm depth (*black lines*) or 5 cm depth (*gray lines*), (**d**) snow water equivalence (SWE, *open circles*, left axis) and snow depth (right axis) measured at the SNOTEL site (*black circles*) or hand-dug pits (*squares*), (**e**) [CO_2] within the litter, snowpack, and air at −3 cm (litter), 0 cm (litter surface), 20, 40, 60, 80, 100, and 120 cm (snowpack or air), darkest color at −3 cm, and lightest gray at 120 cm, (**f**) $\delta^{13}C$ of CO_2 at the same locations (coloring the same as panel e)

liquid water around day 75 (Fig. 4c). This initial melt was followed by colder days and cessation of the short-term melt, then the melt began without interruption around day 115. Snow depth peaked at 130–140 cm, and peak SWE was 45.5 cm on day 117 (39% greater than the long term average).

The permeability of snow to gas transport is a strong function of density (Albert and Shultz 2002). Individual density measurements ranged from 50 g l^{-1} after new snowfall to 483 g l^{-1} during snow melt. Volume-weighted mean snowpack density was generally 250–350 g l^{-1} before day 115, with peaks of 420–430 g l^{-1} during the melt periods (density data not shown, depth shown in Fig. 4d). Kinetic or depth hoar grains were common in the bottom 40 cm of the snowpack.

Observed CO_2 mole fractions within the litter and at the litter surface varied from 1,500 to 3,500 μmol mol^{-1}, about 4 to 9 times higher than ambient mole fractions. Within the snow, mole fractions ranged from ambient to as high as 3,000 μmol mol^{-1}, depending on depth. These observations are similar in magnitude to those made in this and other nearby subalpine forests (Massman and Frank 2006; Mast et al. 1998; Monson et al. 2006a; Sommerfeld et al. 1993), and provide additional evidence of the presence of microbial activity under winter snowpacks. The $\delta^{13}C$ of CO_2 varied from ambient (near −8.1‰) to a minimum of around −22‰, with the most negative values observed in the litter. These isotopic data are comparable to those reported by Brooks et al. (2005) for subalpine conifer and aspen forests in the region. Values of $\delta^{13}C$ observed in the snowpack were not as negative as respiration in this forest based on summertime observations (Fig. 1). δ_R for this forest during summer periods is in the range −24 to −28‰ (Alstad et al. 2007; Bowling et al. 2005; Schaeffer et al. 2008). The isotopic difference between observations of $\delta^{13}C$ in the snowpack and the likely respiratory source is caused by two factors, mixing with air (which could be purely diffusive or partially advective) and diffusive fractionation.

Isotopic mixing relationships

There was a general increase in CO_2 in the litter and in the snowpack around day 75, coincident with the warming and initial melt (Fig. 4e). To first order, CO_2 and $\delta^{13}C$ were inversely correlated, as is frequently observed in forest air (Flanagan et al. 1996). However, there was a marked departure from this pattern at higher values of CO_2; the increase in CO_2 around day 75 was not accompanied by a decrease in $\delta^{13}C$ (Fig. 4f).

The nonlinear mixing relationship (Fig. 2a) provides an explanation for the relatively small change in $\delta^{13}C$ at higher CO_2. Data from both profiles are shown compared to some reasonable expectations for mixing lines in Fig. 5. Profile 1 usually had lower CO_2 at the same heights than profile 2 (Fig. 5 inset) and snow temperature on profile 1 was more directly coupled to air temperature (data not shown). In general the observations conform to expectations based on mixing of air and a respiratory source combined with enrichment by diffusion (Fig. 2). Shown for comparison in Fig. 5 are the $\delta^{13}C$ values of various bulk organic components of the soil at the Niwot Ridge forest (Schaeffer et al. 2008). The lower mixing line was arbitrarily drawn between the bulk litter $\delta^{13}C$ (−26.0‰) and the air, which is the expected mixing line if $\delta^{13}C$ of CO_2 produced by soil respiration was identical to that of the bulk litter, and there was no diffusive enrichment. The observed range of data implies that there is variability in $\delta^{13}C$ of respiration or the influence of diffusion or both.

The isotopic composition of the CO_2 produced during respiration is variable for a variety of reasons (Bowling et al. 2008). For example, $\delta^{13}C$ of respiratory CO_2 during decomposition of conifer needles often changes from initially more depleted to more enriched than the bulk material as mass is lost (Fernandez et al. 2003), and root respiration is generally depleted relative to root biomass (Klumpp et al. 2005; Schnyder and Lattanzi 2005). Given the observations shown in Fig. 5, the $\delta^{13}C$ of the soil respiratory source in our study could not be consistently more negative than the lower bound shown by the solid line, implying a respiratory source of −26.0‰ at a minimum. Since the diffusive fractionation is 4.4‰, the two lines in Fig. 5 are separated by 4.4‰ at the *y*-axis (assuming the $\delta^{13}C$ of the respiratory source is constant, which is addressed below). Our placement of these lines is arbitrary, and since the vertical range in the observations is less than 4.4‰, the lines could together be shifted upward by perhaps 2‰ at the *y*-axis and still bracket the data. Applying this shift would imply a respiratory source of −24‰ and would indicate that the 4.4‰ enrichment was not usually fully present (indicating the dominance of advection).

When all the data in Fig. 5 were combined on a single Keeling plot, the intercept was −22.65 ± 0.01‰ (n = 13,807). Simply subtracting 4.4‰

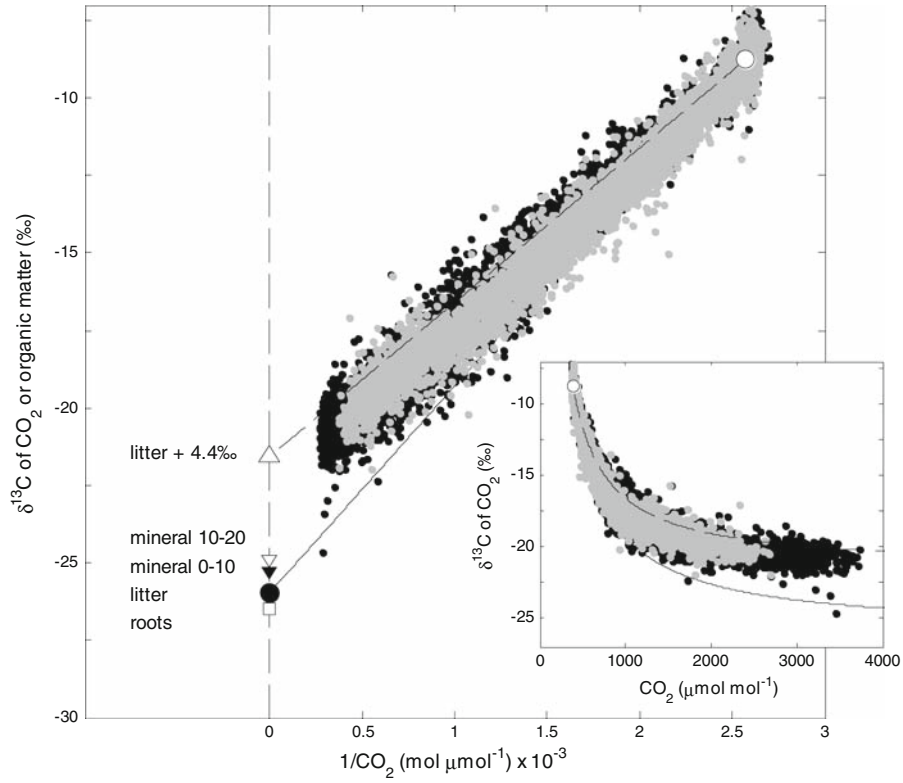

Fig. 5 Keeling-type plot for CO_2 measured within the snowpack, litter, and air (*main panel*) or the same relationship showing the measured quantities (*inset*). Compare to the theoretical relationship in Fig. 2. Time series of the CO_2 and $\delta^{13}C$ data are shown in Fig. 4e, f. All data over the full study period are shown ($n = 6{,}916$ for profile 1, gray circles and $n = 6{,}891$ for profile 2, small black circles). Air (*open circle*), respiratory source (*black circle*), and 4.4‰ enriched respiratory source (*open triangle*) and their respective mixing lines are the same as in Fig. 2. Values of $\delta^{13}C$ of bulk organic material from the site (Schaeffer et al. 2008) are shown for comparison (roots: *open square*, litter: *black circle*, mineral soil 0–10 cm: *black down triangle*, mineral soil 10–20 cm: *open down triangle*). For illustration purposes, the $\delta^{13}C$ of the total respiratory source and the bulk litter are drawn as identical on this plot (*black circle*), but this is not necessarily the case

would imply an average respiratory source of −22.65 to 4.4 = −27.05‰. However, this is incorrect since it would mean 50% of observations (those above the regression line) were more than 4.4‰ enriched above the source, which cannot occur by diffusion. Based on these arguments we estimate the average $\delta^{13}C$ of soil respiration below the snowpack at Niwot Ridge during this study was −26 to −24‰, which is very similar to whole-forest respiration at this site in summer (Alstad et al. 2007; Bowling et al. 2005; Schaeffer et al. 2008) and to the extant carbon stocks in the soil (Fig. 5). We are uncomfortable trying to constrain it further because the observed ranges in $\delta^{13}C$ vary less than the expected 4.4‰ difference between the mixing lines. Combination of these data with a transport model including diffusion, advection, dispersion, and pressure fluctuation influences (e.g., Massman 2006) might provide a way to assess the $\delta^{13}C$ of the soil respiratory source with more confidence.

A further point deserves clarification. Brooks et al. (2005) convincingly demonstrated that winter microbial activity from subalpine soils under snow was carbon limited. Lacking sufficient data to suggest otherwise, they conservatively (but incorrectly) interpreted their CO_2 isotope data by subtracting 4.4‰ from $\delta^{13}C$ measured within the snowpack to obtain the $\delta^{13}C$ of respiratory CO_2. Cerling and colleagues (1991) noted that "the $\delta^{13}C$ of soil CO_2 is always *at least* 4.4‰ enriched relative to the $\delta^{13}C$ for soil respired CO_2", but it can be substantially greater than 4.4‰ as shown by Davidson (1995). The

fractionation associated with diffusive transport is based on the difference in the binary diffusivities of $^{16}O^{12}C^{16}O$ and $^{16}O^{13}C^{16}O$ in air and is 4.4‰, based on theory of kinetic motion of molecules. It is clear from Fig. 5 that the $\delta^{13}C$ of CO_2 in the snow and soil is not simply the isotope ratio of the respiratory source plus 4.4‰; in fact it varies by 15‰ and is highly dependent on CO_2. Under conditions of purely diffusive transport (no advection), if the snow–air interface boundary condition were at 380 μmol mol^{-1} and −8.1‰, the isotope ratio of the CO_2 in the snow must vary between that of the respiratory source and −8.1‰. Hence, while the $\delta^{13}C$ of soil CO_2 is indeed enriched by diffusion relative to the respiratory source, the difference between them can be substantially greater than 4.4‰ due to the atmospheric boundary condition. In order to ascertain the true $\delta^{13}C$ of respiration, mixing relationships such as Eq. 2 or a Keeling plot at multiple depths and then subtracting 4.4‰ should be used (see Methods). Note, however, that this is further complicated by advection as we will show. Hence the conclusions of Brooks et al. (2005) regarding the relative amounts of winter respiration from decomposition versus added sugar (in their Table 1) should be interpreted with caution.

The $\delta^{13}C$ of the apparent respiratory source (δ_{R*}, derived from Keeling plots) was not constant during the study; variability within the overall data envelope shown in Fig. 5 occurred over time. The intercepts of mixing relationships for profile 2 are shown versus time in Fig. 6. $\delta_{R*,c}$ calculated on a 3 h basis varied from −23.8 to −20.8‰ (Fig. 6a), with a distinct periodicity on the order of a few days. This range (less than 2‰ during snow cover, Fig. 6a) was smaller than 4.4‰ (also see Fig. 7b, which shows how the variability compares to the overall magnitude of influence of diffusion). The periodicity was quite similar when $\delta_{R*,c}$ was calculated over longer periods (Fig. 6b, e), with some time-dependent features still present when $\delta_{R*,c}$ was computed on 1 to 4 d periods (such as the dip around day 60–65).

Two assumptions of the Keeling plot approach are that 1) the $\delta^{13}C$ of each source does not change over the time period analyzed (a steady-state assumption), and that 2) only two sources mix. Similarity of the 3, 6, and 12 h plots in Fig. 6 lends some validity to the steady-state assumption, at least for the apparent respiratory source inferred from snowpack observations. The second assumption is more problematic, since $\delta^{13}C$ of root and heterotrophic respiration are likely different (Böstrom et al. 2007; Bowling et al. 2008; Fernandez et al. 2003; Klumpp et al. 2005), and since $\delta^{13}C$ of soil respiration can change over time scales of a few days (Ekblad and Högberg 2001), at least in the summer. The variability in $\delta_{R*,c}$ shown in Fig. 6 may be due to changes in biological activity or changes in transport (or both) as discussed in the next sections.

Biological influences

There were at least two opportunities where one might expect changes in the isotopic composition of soil respiration during our study. The first was a possible change in microbial activity during the midwinter temporary melt period, and the second was the initiation of net carbon gain by the trees in the forest.

There is an active subnivean microbial community in subalpine forests of the region (Brooks et al. 2005; Mast et al. 1998; Monson et al. 2006b; Musselman et al. 2005). Sucrose in the soil solution and microbial biomass are high in winter at the Niwot Ridge forest (Scott-Denton et al. 2006), and the identity of the microbial community differs in these seasons (Lipson 2007). Further, there are high levels of activity of many extracellular enzymes involved in decomposition in winter (Weintraub et al. 2007). In nearby tundra soils, the under snow microbial community is primarily fungal (Schadt et al. 2003), and there are indications this may be true in our study forest as well. Recent work has identified a cold-active fungal community that forms hyphal mats at the litter-snow surface (Schmidt et al. 2008; Schmidt et al. in review (part of the White on Green special issue)). These organisms exhibit very high growth rates at cold temperature and are thought to take advantage of the flush of substrates available in late winter.

Mineral soil temperature was >0°C during the entire study, and there was at least some liquid water available for microbial activity all winter. The midwinter melt period around day 75 led to increases in soil water availability and soil and litter temperature (Fig. 4a–c). This was accompanied by a sustained increase in CO_2 within the litter and snowpack (Fig. 4e), which we interpret as enhanced microbial activity. (Note that CO_2 could also increase

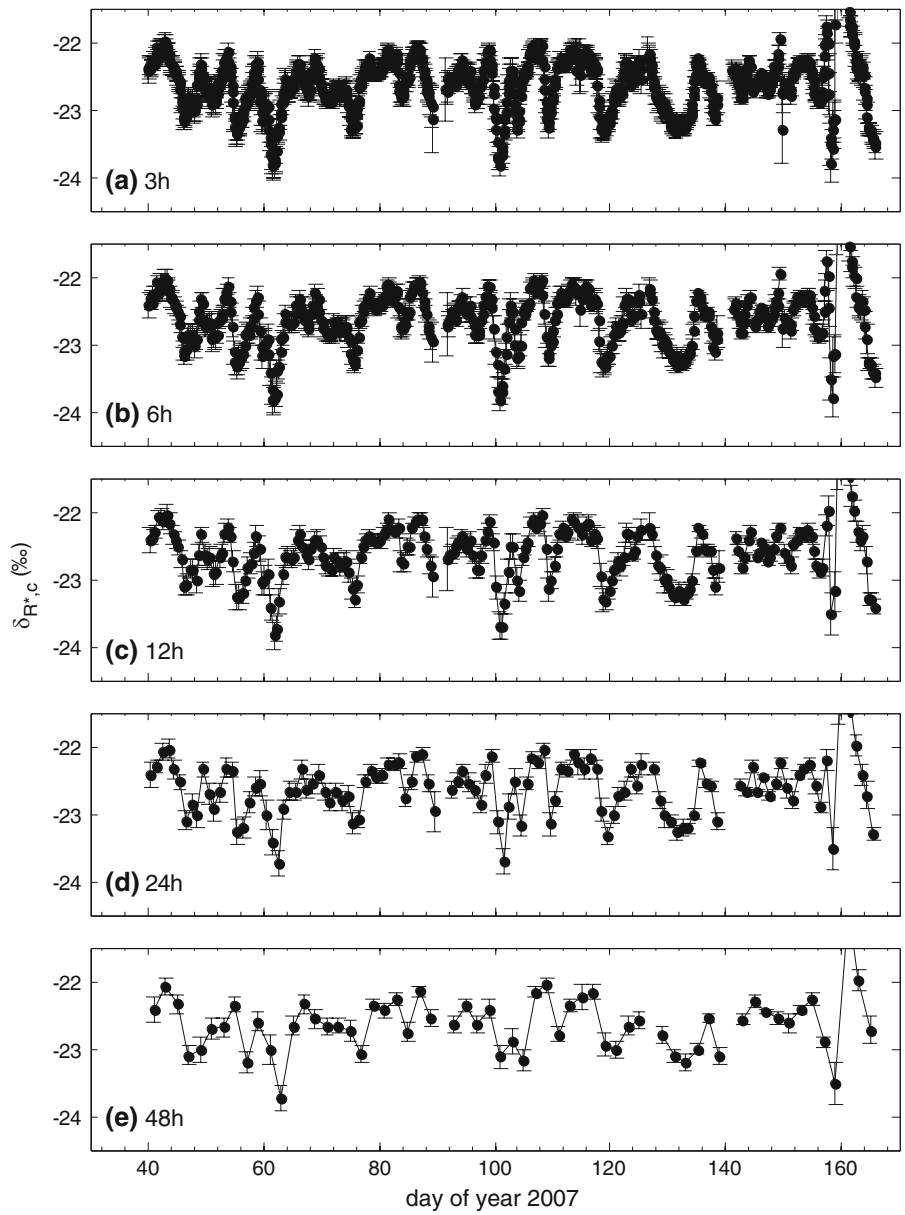

Fig. 6 Time dependence of isotopic mixing relationships within the snowpack. Intercepts ($\delta_{R^*,c}$) of a Keeling mixing line with all inlets from profile 2 (air, snow, litter surface, and litter) calculated on time scales varying from 3 h (one complete cycle through all inlets) to 4 days, plotted over the duration of the study. Time scales are indicated on each panel and data are plotted at the midpoint of the time period. For example, on day 100, panel (**a**) shows eight Keeling plot intercepts calculated every 3 h, and panel (**e**) shows a single Keeling plot intercept calculated from days 98–102. Error bars are the standard error of the intercept

due to increased root respiration, reductions in permeability of the snowpack, or displacement of soil CO_2 by infiltrating melt water). Several other studies have inferred increased microbial activity under snow during melt periods (Brooks et al. 1996; Monson et al. 2006a; Musselman et al. 2005), although some have observed smaller CO_2 fluxes during melt due to reduced diffusion and possibly poor aeration (Hardy et al. 1995; Mast et al. 1998).

Different organic materials in the soil have different bulk $\delta^{13}C$, and if a new substrate became available due to changing temperature or moisture,

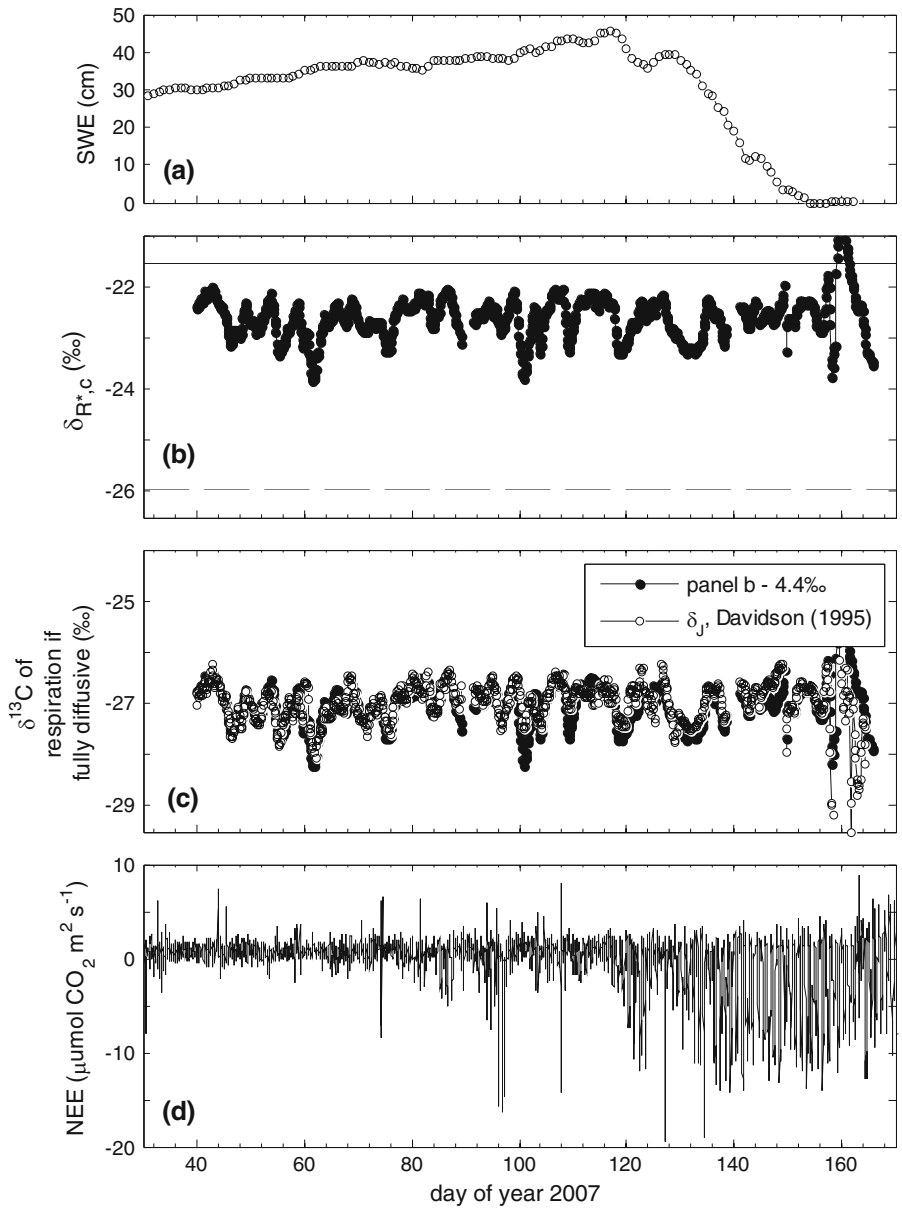

Fig. 7 (**a**) Snow water equivalence (as in Fig. 4 panel **d**), (**b**) 3 h Keeling plot intercepts from profile 2 ($\delta_{R^*,c}$ as in Fig. 6 panel **a**), (**c**) estimates of the $\delta^{13}C$ of respiration obtained by subtracting 4.4‰ from the data in panel (**b**) or from Eq. 2, and (**d**) net ecosystem exchange of CO_2 at 21.5 m measured by eddy covariance. Horizontal lines in (**b**) show $\delta^{13}C$ of the bulk litter (*dashed*) and an enrichment of 4.4‰ above it (*solid*) as in Fig. 5

one might expect changes in $\delta^{13}C$ of respiration. High soil moisture coupled with high respiration during the late spring melt could have led to anaerobic conditions in the soils and associated shifts to a more anaerobic microbial community. There is some evidence that different fungal groups have systematically different $\delta^{13}C$ in their respiration (Böstrom et al. 2007). Despite the strong possibility of microbial responses to the midwinter and spring melts, we did not observe clear changes in the $\delta^{13}C$ of the apparent respiratory source (Fig. 7b). This assertion is complicated by the fact that there was variability in $\delta_{R^*,c}$, but as we show below that variability is probably driven by transport.

We anticipated a possible isotopic change in soil respiration during the transition from a fully respiratory forest in midwinter to the initiation of net carbon uptake (Fig. 7). Although there were short periods of net uptake after the early melt (e.g. days 90–100), substantial carbon uptake began during the full melt period, which is common for this forest (Monson et al. 2005). It is possible that enhanced root activity

would occur in late spring, perhaps associated with ion uptake or regrowth of fine roots damaged by soil heaving (Scott-Denton et al. 2006). The $\delta^{13}C$ of root respiration is thought to differ systematically from that of total soil respiration (Bowling et al. 2008; Klumpp et al. 2005). There was not a clear change in $\delta_{R*,c}$ as net uptake began (Fig. 7b, c). This is an indication that CO_2 produced by root processes during the winter–spring transition did not have a unique $\delta^{13}C$ signature associated with it, unless it was masked by transport. Despite the time-dependent variability (Fig. 7b), our results provide some limited evidence that δ_R of soil respiration in winter, on average, may not be substantially different than in summer in temperature coniferous forests. If this is generally true, it may indicate that seasonal changes in δ_R can be ignored by large-scale carbon cycle modelers, but more work will be necessary to reach this conclusion with confidence.

Following complete snow melt (days 155–170) $\delta_{R*,c}$ showed large excursions in both directions (at this point $\delta_{R*,c}$ was calculated from litter and air measurements as the snow was gone). The negative trend (days 155–160) was probably caused by high winds as discussed below. Causes for the positive trend are unknown but possibilities include a change in diffusive enrichment in the saturated wet soil environment, or possible microbial decomposition of the fungal mat biomass, which dies once the snow melts and is likely to be enriched relative to the litter (see discussion in Bowling et al. 2008 and references therein). It is likely that some CO_2 within the snowpack dissolves in melt water via the carbonate reactions (Solomon and Cerling 1987), and there is a well-known isotopic effect associated with them (Zhang et al. 1995). Additionally, dissolved organic carbon during the melt period in this forest leaches to nearby streams (Hood et al. 2003), leading to possible changes in substrate availability and isotopic content for microbial respiration in the soil and litter during melt. At present the role these processes might play in the temporal dynamics of CO_2 isotopes observed in our study is unknown.

Described in the Methods section were two approaches that, under conditions of fully diffusive transport, allow estimation of the $\delta^{13}C$ of soil respiration. These include the Keeling plot approach (subtracting 4.4‰ from the intercept) and the use of Eq. 2, and the results are compared for profile 2 in Fig. 7c. The two approaches provide similar estimates of the $\delta^{13}C$ of soil respiration, with similar time-dependent variability. The mean is more negative than our estimated range of −26 to −24‰ based on Fig. 5. The results in Fig. 7c are probably systematically biased (too negative) due to the presence of advection, as we show in the next section. However, either approach could potentially be used in manipulative experiments where treatments are compared, provided the influence of advection on treatments and controls did not differ (as would be the case if the snow was physically disrupted by digging for example).

Transport influences

The isotopic influence of diffusion was not equally present at all depths. The isotopic composition of CO_2 in the snowpack and in the soil vary with height (Fig. 4f) because (1) CO_2 is produced primarily at the bottom of the snowpack (within the litter and the soil) and removed primarily by transport at the top, and (2) diffusion enriches the transient pool of CO_2 during transport. Shown in Fig. 8 are daily calculations of δ_{R*} made in three ways (see Fig. 3): first ($\delta_{R*,a}$), with snow and air inlets only, second ($\delta_{R*,b}$), with snow, air, and litter surface inlets, or third ($\delta_{R*,c}$), with snow, air, litter surface, and litter inlets. Those Keeling plots which included observations at greater depths tended to have more enriched (less negative) intercepts. This was true for both profiles, and remained so even as $\delta_{R*,c}$ varied through time (Fig. 8a, b). This effect was especially apparent when the data were examined on a 1:1 basis (Fig. 8c–f), with depth-based differences generally greater at the more negative values of $\delta^{13}C$. We interpret this pattern as a competition between the primary transport mechanisms of diffusion and advection (in this case ventilation of the snowpack with low-CO_2 air from above). If advection events do not completely ventilate the snowpack, then one might expect that the diffusive fractionation would be maximal at the greatest depth, and that advection would remove the diffusive influence to a greater extent at shallower depths. Fig. 8 provides evidence for this assertion.

Transport of heat and mass within snowpacks and firn can be influenced by wind, a phenomenon often called wind pumping or pressure pumping (Albert 2002; Albert and Hardy 1995; Kelley et al. 1968;

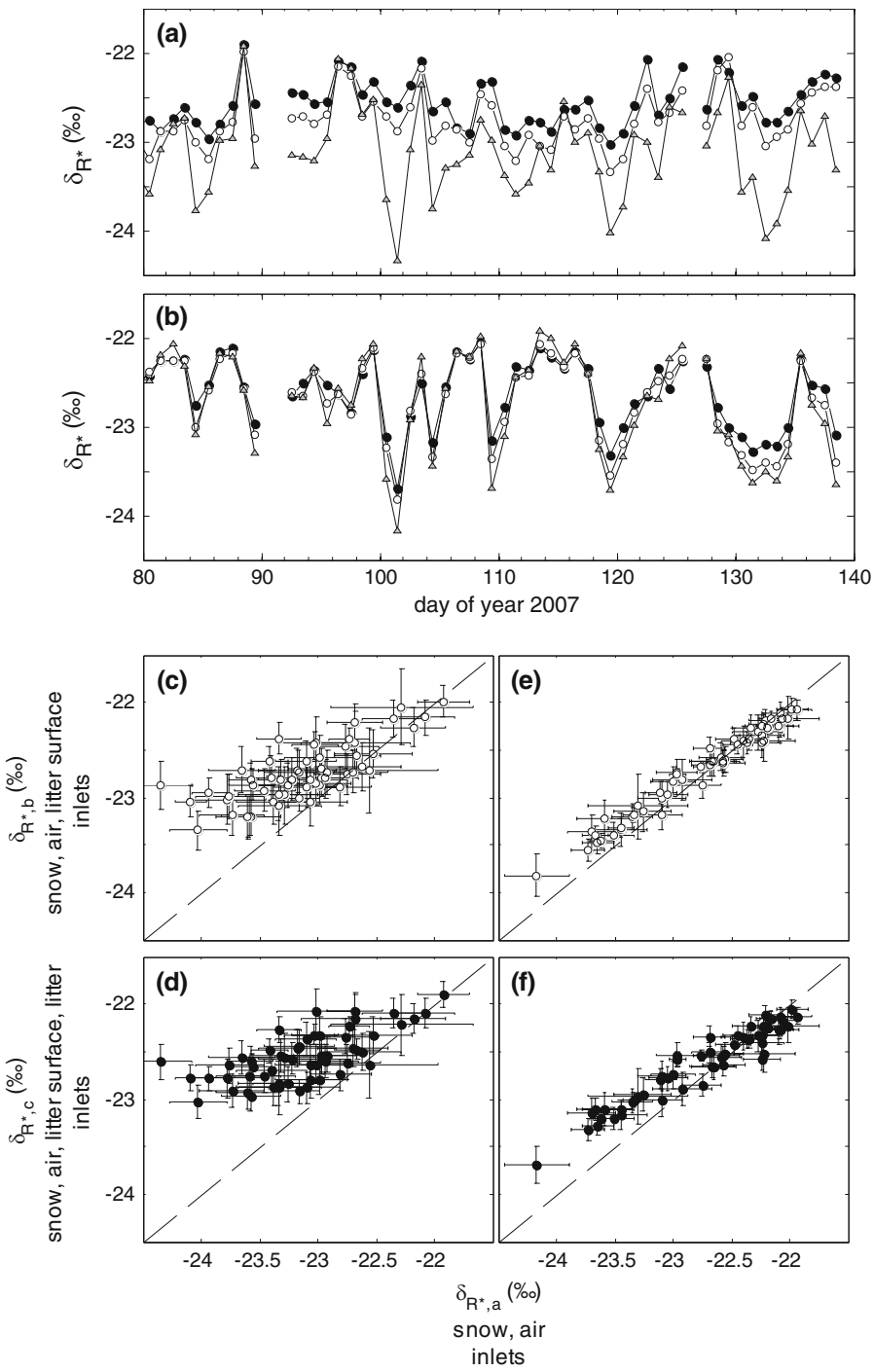

Fig. 8 Depth dependence of the diffusive isotope enrichment during days 80–140. (**a**) 24 h Keeling plot intercepts from profile 1, calculated using only air and snowpack inlets ($\delta_{R^*,a}$, *triangles*), using air, snowpack, and litter surface inlets ($\delta_{R^*,b}$, *open circles*), or using air, snowpack, litter surface, and within-litter inlets ($\delta_{R^*,c}$, *black circles*). (**b**) same as panel **a** but for profile 2. The lower 4 panels show the same data plotted in 1:1 fashion, with the air/snowpack values ($\delta_{R^*,a}$) on the abscissa, and the air/snowpack/litter surface ($\delta_{R^*,b}$ panels **c** and **e**, *open circles*) or air/snowpack/litter surface/litter values ($\delta_{R^*,c}$, panels **d** and **f**, *black circles*) on the ordinate. Panels **c** and **d** are for profile 1, panels **e** and **f** are for profile 2. Error bars are omitted in (**a**) and (**b**) for clarity but shown in the lower panels

Massman and Frank 2006; Monson et al. 2006a; Sturm and Johnson 1991; Suzuki et al. 2006; Takagi et al. 2005). The time-dependent isotopic changes in Figs. 6 and 8 are related to wind as well. Shown in Fig. 9 are 20-day time series of CO_2, $\delta_{R^*,c}$, wind, and pressure. During this period there were several periods of sustained high winds, with horizontal wind speed above the canopy reaching 10–15 m/s for several days (Fig. 9c). Windy periods were often accompanied by large decreases in CO_2 at most

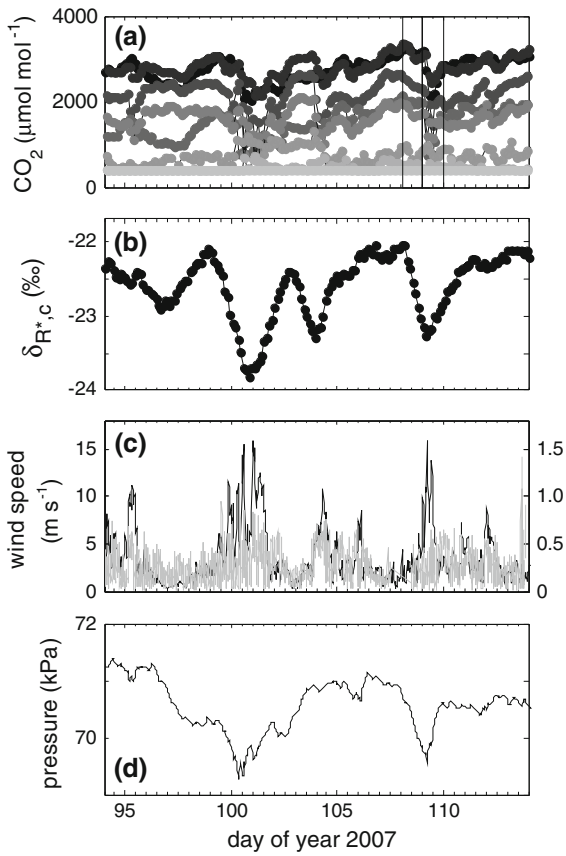

Fig. 9 Influence of wind and pressure on CO_2 and isotopic mixing relationships within the snowpack. (**a**) CO_2 at depths from −3 to 120 cm (dark to light colors respectively). The vertical lines highlight days 108 and 109 which are shown in detail in Fig. 10. (**b**) 3 h Keeling plot intercepts for profile 2 (all inlets, $\delta_{R^*,c}$, see Fig. 6a for error bars), (**c**) horizontal wind speed at 21.5 m (*black line*, left axis) and 2.5 m (*gray line*, right axis), and (**d**) barometric pressure at 12 m

depths (Fig. 9a), and by fairly substantial isotopic changes (Fig. 9b). High wind speed generally led to more negative $\delta_{R^*,c}$. Correlations between $\delta_{R^*,c}$, wind speed, and pressure are listed in Table 2. When the entire time period was analyzed, there were weak but statistically significant correlations between $\delta_{R^*,c}$ and wind speed both above and below canopy for each profile, but there was not a correlation between $\delta_{R^*,c}$ and atmospheric pressure. Other studies have reported correlations between CO_2 and wind speed, but poor correlation with pressure, in soil gas along fault zones (Lewicki et al. 2003) and in snowpacks (Massman and Frank 2006). Using a non-harmonic spectral analysis, Massman and Frank found that the primary CO_2 forcing in a Wyoming forest snowpack was associated with atmospheric motions with periods greater than 3.7 days. They observed time lags of several hours to days between the atmospheric forcing and the CO_2 response, speculating that this was caused by synoptic motions interacting with local terrain features such as nearby mountain peaks and local forest features. The Niwot Ridge study site is similar to theirs and so similar features of wind/pressure forcing may be present.

When analyzed in 10-day periods, there were strong and highly significant correlations, with coefficients of correlation as high as 0.8 (Table 2). Significant correlations with wind speed were always negative, meaning that high wind speed led to more negative $\delta_{R^*,c}$. Strong positive and negative correlations were observed with pressure—this is not surprising since either rapidly increasing or decreasing synoptic pressure leads to high wind and localized pressure gradients. In general, correlations with above-canopy wind speed were greater than below-canopy wind speed or pressure. Note that during periods of snowmelt and increased snow density (days 80–100 and 140–170, see Fig. 4) the pressure pumping influence was decreased (relationships in Table 2 were non-significant). Several researchers (Brooks et al. 1997; Mast et al. 1998; Winston et al. 1995) have noted that gas fluxes are affected when melt water (or resulting ice crusts) within the snowpack influence permeability. The lack of significant wind influence on the isotopic composition of CO_2 within the snowpack during melt periods (Table 2) suggests that gas transport was influenced by some combination of ice lenses and water in the pack. Biological processes were potentially also affected by the increases in soil moisture caused by the draining snowpack.

The negative correlation between $\delta_{R^*,c}$ and wind can be explained as follows. Shown in Fig. 10 are profiles of CO_2, $\delta^{13}C$, and their mixing relationships before and during the wind event on day 109 (also highlighted in Fig. 9a). The sustained high wind caused a significant decrease in CO_2 below 80 cm depth, with reductions in excess of 500 μmol mol^{-1}, even within the litter (Fig. 10a). There was not a concomitant change in $\delta^{13}C$ at these depths (Fig. 10b), but there was a small decrease at 60 and 80 cm. The change was caused by ventilation with forest air with CO_2 of 380 μmol mol^{-1} and $\delta^{13}C$ of −8.1‰ (Fig. 4e, f), which led to a large decrease in

Table 2 Correlations between $\delta_{R^*,c}$ (calculated using air, snow, litter surface, and litter inlets every 3 h) and mean wind speed (u) at 21 m or 2 m height, and with barometric pressure (P) at 12 m

	Start day	End day	u 21 m			u 2 m			P 12 m		
			r	*p*	*n*	*r*	*p*	*n*	*r*	*p*	*n*
Profile 1	40	167	−0.24	0.000*	956	−0.17	0.000*	876	0.03	0.421	956
	40	50	**−0.50**	**0.000***	80	−0.33	0.003	80	−0.13	0.260	80
	50	60	−0.09	0.433	80	−0.10	0.402	80	−0.07	0.564	80
	60	70	0.30	0.007	80	0.02	0.844	80	**−0.54**	**0.000***	80
	70	80	0.05	0.655	80	−0.14	0.313	52	−0.22	0.045	80
	80	90	−0.04	0.731	75	−0.44	0.001*	58	**−0.51**	**0.000***	75
	90	100	−0.34	0.005	68	−0.16	0.189	68	0.00	0.988	68
	100	110	−0.03	0.759	80	−0.13	0.283	73	−0.40	0.000*	80
	110	120	0.03	0.775	79	−0.09	0.430	72	−0.09	0.437	79
	120	130	−0.03	0.795	72	0.04	0.748	72	0.07	0.546	72
	130	140	−0.27	0.023	69	0.16	0.230	59	−0.04	0.727	69
	140	150	0.13	0.301	65	−0.02	0.903	56	−0.46	0.000*	65
	150	160	**−0.58**	**0.000***	80	−0.12	0.307	78	**0.73**	**0.000***	80
	160	167	−0.18	0.229	48	0.11	0.437	48	−0.18	0.232	48
Profile 2	40	167	−0.39	0.000*	953	−0.23	0.000*	875	0.10	0.002	953
	40	50	−0.44	0.000*	80	−0.01	0.908	80	0.14	0.217	80
	50	60	**−0.57**	**0.000***	80	−0.43	0.000*	80	**0.58**	**0.000***	80
	60	70	**−0.69**	**0.000***	80	−0.20	0.076	80	**0.62**	**0.000***	80
	70	80	**−0.60**	**0.000***	80	0.14	0.324	52	−0.46	0.000*	80
	80	90	−0.30	0.011	74	−0.21	0.123	57	−0.02	0.888	74
	90	100	0.00	0.982	68	−0.03	0.814	68	−0.09	0.487	68
	100	110	**−0.71**	**0.000***	80	−0.32	0.007	73	**0.73**	**0.000***	80
	110	120	−0.16	0.158	77	−0.23	0.051	72	**−0.80**	**0.000***	77
	120	130	−0.39	0.001*	72	**−0.61**	**0.000***	72	**−0.65**	**0.000***	72
	130	140	**−0.57**	**0.000***	69	−0.21	0.115	59	−0.12	0.312	69
	140	150	−0.23	0.066	65	−0.02	0.865	56	0.06	0.623	65
	150	160	−0.47	0.000*	80	−0.29	0.011	78	0.22	0.051	80
	160	167	−0.23	0.120	48	0.04	0.798	48	−0.25	0.082	48

Pearson product-moment coefficients (r) and the number of 3 h periods (n) are shown. The probability of a significant correlation (p) was calculated with a t-test with $n - 2$ degrees of freedom. Values with $p \leq 0.001$ are highlighted with an asterisk, and those with $|r| \geq 0.5$ are shown in bold. Statistics were applied to the entire data set or to 10-day periods separately

CO_2, and flushing out of diffusively-enriched CO_2. Note that the mixing relationships shown in Figs. 2 and 5 represent mixing of two large sources of CO_2 (respiration from the soil flux and atmospheric CO_2), and a much smaller pool of diffusively-enriched CO_2 (stored within the snowpack). A wind event causes ventilation of the diffusively enriched pool, and the remaining gas is closer to the mixing line between the two sources (the lower line in Figs. 2 and 5). The directional change away from diffusion-dominated transport is evident in Fig. 10c, d. The relative importance of the wind influence compared to the influence of diffusive fractionation can be seen in Fig. 7b. The lower and upper horizontal lines represent the bulk litter $\delta^{13}C$ and enrichment above this value as discussed for Fig. 5. Since the range of the wind-induced changes is smaller than the 4.4‰ enrichment, the dominance of diffusive transport even under very windy conditions is still apparent. These results suggest that the wind influence can maximally remove maybe 20–25 percent of the diffusive enrichment. Again we stress that the

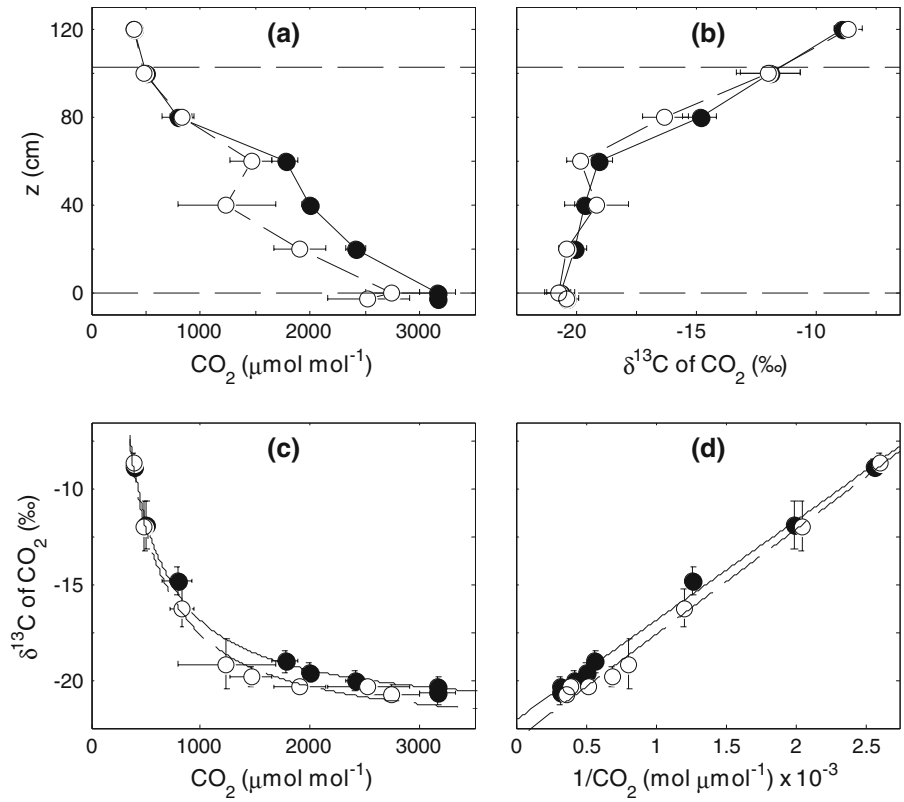

Fig. 10 CO_2 and $\delta^{13}C$ of CO_2 within the snowpack before (*black circles*, day 108) and during (*open circles*, day 109) a major wind event. Vertical profiles of CO_2 (**a**) and $\delta^{13}C$ (**b**) are shown, with the litter surface and the top of the snowpack indicated by dashed horizontal lines. The corresponding relationships between $\delta^{13}C$ and CO_2 (**c**), and the Keeling plots (**d**) are also shown. Lines in panels **c** and **d** are the Keeling mixing lines calculated from the 3 h data (*solid* on day 108 before the wind, *dashed* on day 109 during the wind). Data shown are means and standard deviations of eight 3-h measurements made over each 24 h period. CO_2 data for these days are highlighted in Fig. 9. Regression lines in (**d**) are $y = 5219x - 22.07$, $r^2 = 0.996$ (before), and $y = 5488x - 23.08$, $r^2 = 0.993$ (after)

placement of the horizontal lines in Fig. 7b is arbitrary, so the distance of the data from one line or the other does not indicate the relative magnitudes of diffusive and advective transport.

Conclusions

We conducted an extensive study of the carbon isotope composition of CO_2 within a subalpine forest snowpack during winter and through the spring melt. We found evidence of microbial activity under the snowpack, adding to the array of studies showing that substantial respiratory activity occurs in winter. The isotopic composition of soil respiration at the Niwot Ridge forest in winter is in the range of −26 to −24‰, which is similar to that of the extant litter and to whole-forest respiration in summer. There was a midwinter period of melt that increased soil temperature and added liquid water to soils, but there was not an obvious change in $\delta^{13}C$ of beneath-snow respiration associated with this event, nor did we find an isotopic change upon initiation of net carbon uptake by the forest. The $\delta^{13}C$ of the apparent respiratory source was strongly influenced by wind speed, particularly above the canopy. Strong wind events led the apparent respiratory source in the snowpack to become more negative (less enriched in ^{13}C). Trace gas transport in this snowpack was dominated by diffusion with short-term variability driven by advection. The influence of diffusion was differentially apparent at greater depths. Physical factors influencing gas transport appeared to dominate over biological factors in their effects on $\delta^{13}C$ of CO_2 within this subalpine forest snowpack.

Acknowledgements Data from this project are available for collaborative use by anyone interested—contact the senior author. Kurt Chowanski, Lucas Zukiewicz, and Dave Millar of the University of Colorado Mountain Research Station and Niwot Ridge Long-Term Ecological Research (LTER) project helped maintain the TDL in the field, and these folks plus Ken Hill and Scott Jackson dug the snow pits. Thanks to Sarah Gaines and Andy Schauer for preparation and measurement of calibration gases at the Stable Isotope Ratio Facility for Environmental Research at the University of Utah, and to Chris Landry of the Center for Snow and Avalanche Studies and Bert Tanner of Campbell Scientific for helpful discussions regarding snow temperature measurement. We thank Paul Brooks, Thure Cerling, and Andrew Moyes for helpful discussions and comments on an early draft. We are grateful to the USDA Natural Resources Conservation Service, Colorado Snow Survey Program for maintaining the SNOTEL network and freely sharing their data for this study. This research was supported by a grant to DRB from the Office of Science (BER), U. S. Department of Energy, Grant No. DE-FG02-04ER63904. We acknowledge the additional support of a grant from the National Institute for Climate Change Research (NICCR) Western Section to RKM, and National Science Foundation grant DEB 0423662 to the Niwot Ridge LTER program.

References

Aitchison CW (2001) The effect of snow cover on small animals. In: Jones HG, Pomeroy JW, Walker DA, Hoham RW (eds) Snow ecology: an interdisciplinary examination of snow-covered systems. Cambridge University Press, Cambridge

Albert MR (2002) Effects of snow and firn ventilation on sublimation rates. Ann Glaciol 35:52–56. doi:10.3189/172756402781817194

Albert MR, Hardy JP (1995) Ventilation experiments in a seasonal snow cover. In: Tonnessen KA, Williams MA, Tranter M (eds) Biogeochemistry of seasonally snow-covered catchments. International Association of Hydrologic Sciences Press, Institute of Hydrology, Wallingford, pp 41–49

Albert MR, Shultz EF (2002) Snow and firn properties and air-snow transport processes at Summit, Greenland. Atmos Environ 36:2789–2797. doi:10.1016/S1352-2310(02)00119-X

Alstad KP, Lai C-T, Flanagan LB, Ehleringer JR (2007) Environmental controls on the carbon isotope composition of ecosystem-respired CO_2 in contrasting forest ecosystems in Canada and the USA. Tree Physiol 27:1361–1374

Amundson R, Stern L, Baisden T, Wang Y (1998) The isotopic composition of soil and soil-respired CO_2. Geoderma 82:83–114. doi:10.1016/S0016-7061(97)00098-0

Anthoni PM, Law BE, Unsworth MH (1999) Carbon and water vapor exchange of an open-canopied ponderosa pine ecosystem. Agric For Meteorol 95:151–168. doi:10.1016/S0168-1923(99)00029-5

Assonov SS, Brenninkmeijer CAM, Jockel P (2005) The ^{18}O isotope exchange rate between firn air CO_2 and the firn matrix at three Antarctic sites. J Geophys Res 110: D18310. doi:18310.11029/12005JD005769

Böstrom B, Comstedt D, Ekblad A (2007) Can isotopic fractionation during respiration explain the ^{13}C-enriched sporocarps of ectomycorrhizal and saprotrophic fungi? New Phytol 177:1012–1019. doi:10.1111/j.1469-8137.2007.02332.x

Bowling DR, McDowell NG, Bond BJ, Law BE, Ehleringer JR (2002) ^{13}C content of ecosystem respiration is linked to precipitation and vapor pressure deficit. Oecologia 131:113–124. doi:10.1007/s00442-001-0851-y

Bowling DR, Burns SP, Conway TJ, Monson RK, White JWC (2005) Extensive observations of CO_2 carbon isotope content in and above a high-elevation subalpine forest. Global Biogeochem Cycles 19:GB3023. doi:3010.1029/2004GB002394

Bowling DR, Pataki DE, Randerson JT (2008) Carbon isotopes in terrestrial ecosystem pools and CO_2 fluxes. New Phytol 178:24–40. doi:10.1111/j.1469-8137.2007.02342.x

Brooks PD, Williams MW, Schmidt SK (1996) Microbial activity under alpine snowpacks, Niwot Ridge, Colorado. Biogeochemistry 32:93–113. doi:10.1007/BF00000354

Brooks PD, Schmidt SK, Williams MW (1997) Winter production of CO_2 and N_2O from alpine tundra: environmental controls and relationship to inter-system C and N fluxes. Oecologia 110:403–413

Brooks PD, McKnight D, Elder K (2005) Carbon limitation of soil respiration under winter snowpacks: potential feedbacks between growing season and winter carbon fluxes. Glob Change Biol 11:231–238. doi:10.1111/j.1365-2486.2004.00877.x

Cerling TE, Solomon DK, Quade J, Bowman JR (1991) On the isotopic composition of carbon in soil carbon dioxide. Geochim Cosmochim Acta 55:3403–3405. doi:10.1016/0016-7037(91)90498-T

Chen BZ, Chen JM, Huang L, Tans PP (2006) Modeling dynamics of stable carbon isotopic exchange between a boreal forest ecosystem and the atmosphere. Glob Change Biol 12:1842–1867. doi:10.1111/j.1365-2486.2006.01200.x

Clark ID, Henderson L, Chappellaz J, Fisher D, Koerner R, Worthy DEJ, Kotzer T, Norman AL, Barnola JM (2007) CO_2 isotopes as tracers of firn air diffusion and age in an Arctic ice cap with summer melting, Devon Island, Canada. J Geophys Res 112:D01301. doi:01310.01029/02006JD007471

Coxson DS, Parkinson D (1987) Winter respiratory activity in aspen woodland forest floor litter and soils. Soil Biol Biochem 19:49–59. doi:10.1016/0038-0717(87)90125-8

Davidson GR (1995) The stable isotopic composition and measurement of carbon in soil CO_2. Geochim Cosmochim Acta 59:2485–2489. doi:10.1016/0016-7037(95)00143-3

Edwards AC, Cresser MS (1992) Freezing and its effect on chemical and biological properties of soil. Adv Soil Sci 18:59–79

Ekblad A, Högberg P (2001) Natural abundance of ^{13}C in CO_2 respired from forest soils reveals speed of link between tree photosynthesis and root respiration. Oecologia 127:305–308. doi:10.1007/s004420100667

Farquhar GD, Ehleringer JR, Hubick KT (1989) Carbon isotope discrimination and photosynthesis. Annu Rev Plant Physiol Plant Mol Biol 40:503–537. doi:10.1146/annurev.pp.40.060189.002443

Fernandez I, Mahieu N, Cadisch G (2003) Carbon isotopic fractionation during decomposition of plant materials of

different quality. Global Biogeochem Cycles 17:1075. doi:1010.1029/2001GB001834

Flanagan LB, Brooks JR, Varney GT, Berry SC, Ehleringer JR (1996) Carbon isotope discrimination during photosynthesis and the isotope ratio of respired CO_2 in boreal forest ecosystems. Global Biogeochem Cycles 10:629–640. doi:10.1029/96GB02345

Francey RJ, Allison CE, Etheridge DM, Trudinger CM, Enting IG, Leuenberger M et al (1999) A 1000-year high precision record of $\delta^{13}C$ in atmospheric CO_2. Tellus 51B:170–193

Groffman PM, Hardy JP, Driscoll CT, Fahey TJ (2006) Snow depth, soil freezing, and fluxes of carbon dioxide, nitrous oxide and methane in a northern hardwood forest. Glob Change Biol 12:1748–1760. doi:10.1111/j.1365-2486.2006.01194.x

Hardy JP, Davis RE, Winston GC (1995) Evolution of factors affecting gas transmissivity of snow in the boreal forest. In: Tonnessen KA, Williams MA, Tranter M (eds) Biogeochemistry of seasonally snow-covered catchments. International Association of Hydrologic Sciences Press, Institute of Hydrology, Wallingford, pp 51–59

Hemming D, Yakir D, Ambus P, Aurela M, Besson C, Black K et al (2005) Pan-European $\delta^{13}C$ values of air and organic matter from forest ecosystems. Glob Change Biol 11:1065–1093. doi:10.1111/j.1365-2486.2005.00971.x

Hirano T (2005) Seasonal and diurnal variations in topsoil and subsoil respiration under snowpack in a temperate deciduous forest. Global Biogeochem Cycles 19:GB2011. doi:2010.1029/2004GB002259

Hoham RW, Duval B (2001) Microbial ecology of snow and freshwater ice with emphasis on snow algae. In: Jones HG, Pomeroy JW, Walker DA, Hoham RW (eds) Snow ecology: an interdisciplinary examination of snow-covered systems. Cambridge University Press, Cambridge

Hood E, McKnight DM, Williams MW (2003) Sources and chemical character of dissolved organic carbon across an alpine/subalpine ecotone, Green Lakes Valley, Colorado Front Range, United States. Water Resour Res 39:1188. doi:1110.1029/2002WR001738

Keeling CD (1958) The concentration and isotopic abundances of atmospheric carbon dioxide in rural areas. Geochim Cosmochim Acta 13:322–334. doi:10.1016/0016-7037(58)90033-4

Kelley JJ, Weaver DF, Smith BP (1968) The variation of carbon dioxide under the snow in the Arctic. Ecology 49:358–361. doi:10.2307/1934472

Klumpp K, Schäufele R, Lötscher M, Lattanzi FA, Feneis W, Schnyder H (2005) C-isotope composition of CO_2 respired by shoots and roots: fractionation during dark respiration? Plant Cell Environ 28:241–250. doi:10.1111/j.1365-3040.2004.01268.x

Knohl A, Werner RA, Brand WA, Buchmann N (2005) Short-term variations in $\delta^{13}C$ of ecosystem respiration reveals link between assimilation and respiration in a deciduous forest. Oecologia 142:70–82. doi:10.1007/s00442-004-1702-4

Kueppers LM, Harte J (2005) Subalpine forest carbon cycling: short- and long-term influence of climate and species. Ecol Appl 15:1984–1999. doi:10.1890/04-1769

Lai C-T, Ehleringer JR, Schauer AJ, Tans PP, Hollinger DY, Paw UKT et al (2005) Canopy-scale $\delta^{13}C$ of photosynthetic and respiratory CO_2 fluxes: observations in forest biomes across the United States. Glob Change Biol 11:633–643. doi:10.1111/j.1365-2486.2005.00931.x

Lewicki JL, Evans WC, Hilley GE, Sorey ML, Rogie JD, Brantley SL (2003) Shallow soil CO_2 flow along the San Andreas and Calaveras Faults, California. J Geophys Res 108:2187. doi:2110.1029/2002JB002141

Lipson DA (2007) Relationships between temperature responses and bacterial community structure along seasonal and altitudinal gradients. FEMS Microbiol Ecol 59:418–427. doi:10.1111/j.1574-6941.2006.00240.x

Lipson DA, Monson RK (1998) Plant-microbe competition for soil amino acids in the alpine tundra: effects of freeze-thaw and dry-rewet events. Oecologia 113:406–414. doi:10.1007/s004420050393

Lipson DA, Schmidt SK, Monson RK (2000) Carbon availability and temperature control the post-snowmelt decline in alpine soil microbial biomass. Soil Biol Biochem 32:441–448. doi:10.1016/S0038-0717(99)00068-1

Mariko S, Nishimura N, Mo WH, Matsui Y, Kibe T, Koizumi H (2000) Winter CO_2 flux from soil and snow surfaces in a cool-temperate deciduous forest, Japan. Ecol Res 15:363–372. doi:10.1046/j.1440-1703.2000.00357.x

Massman WJ (2006) Advective transport of CO_2 in permeable media induced by atmospheric pressure fluctuations: 1. An analytical model. J Geophys Res 111:G03004. doi:03010.01029/02006JG000163

Massman WJ, Frank JM (2006) Advective transport of CO_2 in permeable media induced by atmospheric pressure fluctuations: 2. Observational evidence under snowpacks. J Geophys Res 111:G03005. doi:03010.01029/02006JG000164

Massman WJ, Sommerfeld RA, Mosier AR, Zeller KF, Hehn TJ, Rochelle SG (1997) A model investigation of turbulence-driven pressure-pumping effects on the rate of diffusion of CO_2, N_2O, and CH_4 through layered snowpacks. J Geophys Res 102:18851–18863. doi:10.1029/97JD00844

Mast MA, Wickland KP, Striegl RT, Clow DW (1998) Winter fluxes of CO_2 and CH_4 from subalpine soils in Rocky Mountain National Park, Colorado. Global Biogeochem Cycles 12:607–620. doi:10.1029/98GB02313

Matzner E, Borken W (2008) Do freeze-thaw events enhance C and N losses from soils of different ecosystems? A review. Eur J Soil Sci 59:274–284. doi:10.1111/j.1365-2389.2007.00992.x

McDowell NG, Marshall JD, Hooker TD, Musselman R (2000) Estimating CO_2 flux from snowpacks at three sites in the Rocky Mountains. Tree Physiol 20:745–753

McDowell NG, Bowling DR, Schauer A, Irvine J, Bond BJ, Law BE et al (2004) Associations between carbon isotope ratios of ecosystem respiration, water availability and canopy conductance. Glob Change Biol 10:1767–1784. doi:10.1111/j.1365-2486.2004.00837.x

Mikan CJ, Schimel JP, Doyle AP (2002) Temperature controls of microbial respiration in arctic tundra soils above and below freezing. Soil Biol Biochem 34:1785–1795. doi:10.1016/S0038-0717(02)00168-2

Monson RK, Turnipseed AA, Sparks JP, Harley PC, Scott-Denton LE, Sparks K et al (2002) Carbon sequestration in a high-elevation, subalpine forest. Glob Change Biol 8:459–478. doi:10.1046/j.1365-2486.2002.00480.x

Monson RK, Sparks JP, Rosenstiel TN, Scott-Denton LE, Huxman TE, Harley PC et al (2005) Climatic influences on net ecosystem CO_2 exchange during the transition from wintertime carbon source to springtime carbon sink in a high-elevation, subalpine forest. Oecologia 146:130–147. doi:10.1007/s00442-005-0169-2

Monson RK, Burns SP, Williams MW, Delany AC, Weintraub M, Lipson DA (2006a) The contribution of beneath-snow soil respiration to total ecosystem respiration in a high-elevation, subalpine forest. Global Biogeochem Cycles 20:GB3030. doi:3010.1029/2005GB002684

Monson RK, Lipson DL, Burns SP, Turnipseed AA, Delany AC, Williams MW et al (2006b) Winter forest soil respiration controlled by climate and microbial community composition. Nature 439:711–714. doi:10.1038/nature04555

Mortazavi B, Chanton JP, Prater JL, Oishi AC, Oren R, Katul G (2005) Temporal variability in ^{13}C of respired CO_2 in a pine and a hardwood forest subject to similar climatic conditions. Oecologia 142:57–69. doi:10.1007/s00442-004-1692-2

Murayama S, Saigusa N, Chan D, Yamamoto S, Kondo H, Eguchi Y (2003) Temporal variations of atmospheric CO_2 concentration in a temperate deciduous forest in central Japan. Tellus B Chem Phys Meterol 55:232–243. doi:10.1034/j.1600-0889.2003.00061.x

Musselman RC, Massman WJ, Frank JM, Korfmacher JL (2005) The temporal dynamics of carbon dioxide under snow in a high elevation Rocky Mountain subalpine forest and meadow. Arct Antarct Alp Res 37:527–538. doi:10.1657/1523-0430(2005)037[0527:TTDOCD]2.0.CO;2

Nobel PS (2005) Physicochemical and environmental plant physiology. Elsevier Academic Press, Amsterdam

Oechel WC, Vourlitis G, Hastings SJ (1997) Cold season CO_2 emission from arctic soils. Global Biogeochem Cycles 11:163–172. doi:10.1029/96GB03035

Panikov NS, Flanagan PW, Oechel WC, Mastepanov MA, Christensen TR (2006) Microbial activity in soils frozen to below −39 degrees C. Soil Biol Biochem 38:785–794. doi:10.1016/j.soilbio.2005.07.004

Pataki DE, Ehleringer JR, Flanagan LB, Yakir D, Bowling DR, Still CJ, Buchmann N, Kaplan JO, Berry JA (2003) The application and interpretation of Keeling plots in terrestrial carbon cycle research. Global Biogeochem Cycles 17:1022. doi:1010.1029/2001GB001850

Ponton S, Flanagan LB, Alstad KP, Johnson BG, Morgenstern K, Kljun N et al (2006) Comparison of ecosystem water-use efficiency among Douglas-fir forest, aspen forest and grassland using eddy covariance and carbon isotope techniques. Glob Change Biol 12:294–310. doi:10.1111/j.1365-2486.2005.01103.x

Randerson JT, Collatz GJ, Fessenden JE, Munoz AD, Still CJ, Berry JA, Fung IY, Suits N, Denning AS (2002) A possible global covariance between terrestrial gross primary production and ^{13}C discrimination: consequences for the atmospheric ^{13}C budget and its response to ENSO. Global Biogeochem Cycles 16:1136. doi:1110.1029/2001GB001845

Sacks WJ, Schimel DS, Monson RK (2007) Coupling between carbon cycling and climate in a high-elevation, subalpine forest: a model-data fusion analysis. Oecologia 151:54–58. doi:10.1007/s00442-006-0565-2

Schadt CW, Martin AP, Lipson DA, Schmidt SK (2003) Seasonal dynamics of previously unknown fungal lineages in tundra soils. Science 301:1359–1361. doi:10.1126/science.1086940

Schaeffer SM, Anderson DE, Burns SP, Monson RK, Sun J, Bowling DR (2008) Canopy structure and atmospheric flows in relation to the $\delta^{13}C$ of respired CO_2 in a subalpine coniferous forest. Agric For Meteorol 148:592–605. doi:10.1016/j.agrformet.2007.11.003

Schaeffer SM, Miller JB, Vaughn BH, White JWC & Bowling DR (in press) Long-term field performance of a tunable diode laser absorption spectrometer for analysis of carbon isotopes of CO_2 in forest air. Atmos Chem Phys

Schimel JP, Clein JS (1996) Microbial response to freeze-thaw cycles in tundra and taiga soils. Soil Biol Biochem 28:1061–1066. doi:10.1016/0038-0717(96)00083-1

Schindlbacher A, Zechmeister-Boltenstern S, Glatzel G, Jandl R (2007) Winter soil respiration from an Austrian mountain forest. Agric For Meteorol 146:205–215. doi:10.1016/j.agrformet.2007.06.001

Schmidt SK, Lipson DA (2004) Microbial growth under the snow: implications for nutrient and allelochemical availability in temperate soils. Plant Soil 259:1–7. doi:10.1023/B:PLSO.0000020933.32473.7e

Schmidt SK, Wilson KL, Meyer AF, Gebauer MM, King AJ (2008) Phylogeny and ecophysiology of opportunistic "snow molds" from a subalpine forest ecosystem. Microb Ecol. doi:10.1007/s00248-00008-09387-00246

Schmidt SK, Wilson KL, Monson RK, Lipson DA (in review (part of the White on Green special issue)) Exponential growth of "snow molds" at sub-zero temperatures: an explanation for high beneath-snow respiration rates and Q_{10} values. Biogeochemistry

Schnyder H, Lattanzi FA (2005) Partitioning respiration of C3–C4 mixed communities using the natural abundance 13C approach – testing assumptions in a controlled environment. Plant Biol 7:592–600. doi:10.1055/s-2005-872872

Scholze M, Ciais P, Heimann M (2008) Modeling terrestrial ^{13}C cycling: climate, land use and fire. Global Biogeochem Cycles 22:GB1009. doi:1010.1029/2006GB002899

Scott-Denton LE, Rosenstiel TN, Monson RK (2006) Differential controls by climate and substrate over the heterotrophic and rhizospheric components of soil respiration. Glob Change Biol 12:205–216. doi:10.1111/j.1365-2486.2005.01064.x

Solomon DK, Cerling TE (1987) The annual carbon dioxide cycle in a montane soil: observations, modeling, and implications for weathering. Water Resour Res 23:2257–2265. doi:10.1029/WR023i012p02257

Sommerfeld RA, Musselman RC, Reuss JO, Mosier AR (1991) Preliminary measurements of CO_2 in melting snow. Geophys Res Lett 18:1225–1228. doi:10.1029/91GL01502

Sommerfeld RA, Mosier AR, Musselman RC (1993) CO_2, CH_4 and N_2O flux through a Wyoming snowpack and implications for global budgets. Nature 361:140–142. doi:10.1038/361140a0

Sturm M, Johnson JB (1991) Natural convection in the subarctic snow cover. J Geophys Res 96:11657–11671. doi:10.1029/91JB00895

Suits NS, Denning AS, Berry JA, Still CJ, Kaduk J, Miller JB, Baker IT (2005) Simulation of carbon isotope

discrimination of the terrestrial biosphere. Global Biogeochem Cycles 19:GB1017. doi:1010.1029/2003GB002141

Suni T, Berninger F, Vesala T, Markkanen T, Hari P, Makela A et al (2003) Air temperature triggers the recovery of evergreen boreal forest photosynthesis in spring. Glob Change Biol 9:1410–1426. doi:10.1046/j.1365-2486.2003.00597.x

Suzuki S, Ishizuka S, Kitamura K, Yamanoi K, Nakai Y (2006) Continuous estimation of winter carbon dioxide efflux from the snow surface in a deciduous broadleaf forest. J Geophys Res 111:D17101. doi:17110.11029/12005JD006595

Takagi K, Nomura M, Ashiya D, Takahashi H, Sasa K, Fujinuma Y, Shibata H, Akibayashi Y, Koike T (2005) Dynamic carbon dioxide exchange through snowpack by wind-driven mass transfer in a conifer-broadleaf mixed forest in northernmost Japan. Global Biogeochem Cycles 19:GB2012. doi:2010.1029/2004GB002272

Trudinger CM, Enting IG, Etheridge DM, Francey RJ, Levchenko VA, Steele LP et al (1997) Modeling air movement and bubble trapping in firn. J Geophys Res 102:6747–6763. doi:10.1029/96JD03382

Uchida M, Mo W, Nakatsubo T, Tsuchiya Y, Horikoshi T, Koizumi H (2005) Microbial activity and litter decomposition under snow cover in a cool-temperate broad-leaved deciduous forest. Agric For Meteorol 134:102–109. doi:10.1016/j.agrformet.2005.11.003

Weintraub MN, Scott-Denton LE, Schmidt SK, Monson RK (2007) The effects of tree rhizodeposition on soil exoenzyme activity, dissolved organic carbon, and nutrient availability in a subalpine forest ecosystem. Oecologia 154:327–338. doi:10.1007/s00442-007-0804-1

Williams MW, Cline D, Hartman M, Bardsley T (1999) Data for snowmelt model development, calibration, and verification at an alpine site, Colorado Front Range. Water Resour Res 35:3205–3209. doi:10.1029/1999WR900088

Winston GC, Stephens BB, Sundquist ET, Hardy JP, Davis RE (1995) Seasonal variability in CO_2 transport through snow in a boreal forest. In: Tonnessen KA, Williams MA, Tranter M (eds) Biogeochemistry of seasonally snow-covered catchments. International Association of Hydrologic Sciences Press, Institute of Hydrology, Wallingford, pp 61–70

Zhang J, Quay PD, Wilbur DO (1995) Carbon isotope fractionation during gas-water exchange and dissolution of CO_2. Geochim Cosmochim Acta 59:107–114. doi:10.1016/0016-7037(95)91550-D

Zimov SA, Zimova GM, Daviodov SP, Daviodova AI, Voropaev YV, Voropaeva ZV et al (1993) Winter biotic activity and production of CO_2 in Siberian soils: a factor in the greenhouse effect. J Geophys Res 98:5017–5023. doi:10.1029/92JD02473

Zobitz JM, Keener JP, Schnyder H, Bowling DR (2006) Sensitivity analysis and quantification of uncertainty for isotopic mixing relationships in carbon cycle research. Agric For Meteorol 136:56–75

Zobitz JM, Burns SP, Ogée J, Reichstein M, Bowling DR (2007) Partitioning net ecosystem exchange of CO_2: a comparison of a Bayesian/isotope approach to environmental regression methods. J Geophys Res 112:G03013. doi:03010.01029/02006JG000282

Zobitz JM, Burns SP, Reichstein M, Bowling DR (2008) Partitioning net ecosystem carbon exchange and the carbon isotopic disequilibrium between whole-ecosystem photosynthesis and respiration in a subalpine forest. Glob Change Biol 14:1785–1800